KATHOLIEKE HOGESCHOOL
BRUGGE - OOSTENDE

ASSOCIATIE K.U.LEUVEN

Departement Industriële Wetenschappen en Technologie

Opleiding master in de industriële wetenschappen: elektromechanica
Afstudeerrichting luchtvaarttechnologie

Modelling and simulation of the Revolutionary Turbine Accelerator

Eindwerk aangeboden tot het behalen van het diploma van
master in de industriële wetenschappen: elektromechanica

door **Jelle Goyvaerts**

o.l.v Wim Vanparys, KHBO
Guillermo Paniagua, VON KARMAN INSTITUUT
Victor Fernández Villacé, VON KARMAN INSTITUUT

Academiejaar 2008 - 2009

Announcement

“This final year project was an exam. Commentary made during the presentation is not taken into account.”

"Deze eindverhandeling was een examen. De tijdens de verdediging geformuleerde opmerkingen werden niet opgenomen".

Preface

Here I would like to thank everyone who made a contribution to my thesis. Also to all the people I forgot or do not call by name below.

First of all I would like to thank my both VKI promoters. Guillermo Paniagua and Victor Fernández Villacé for their guidance, theoretical support and the help finding the exact information I was searching for. Also thanks to my KHBO promoter, Wim Vanparys who also gave me support, in addition to his clear view on the project and future considerations.

Second I would like to say thank you to Jean-François Herbiet for his EcosimPro help, in which Victor also made his contribution, and for the information about the conical inlet and its implementation.

Without the IT help of Olivier Jadot there would be no EcosimPro at the VKI, on my computer and it definitely would not be accessible at home. Also the people of the VKI library deserve a great thank you for delivering the requested papers as soon as possible which were essential to understand the working principle of the RTA.

Next, a thank you to my VKI-colleagues, Piet Van den Ecker, Marylène Andre and Maarten De Moor for the great time and discussions about the occurring problems. Most of the time they helped me, without them knowing it, determining and resolving the problems. Of course to all the others as well, to keep up the spirit in the little room were we spent our time.

Last I would like to thank Heleen Claes for her grammatical corrections and my parents, who financed my studies, brother and girlfriend Ellen for attentively listening to my experiences, most of the time without understanding what it was all about.

Jelle Goyvaerts,
21st of May 2009

Abstract (English)

In the last decades, a lot of research and development is spent on the reduction of the fuel consumption of commercial airliners without reducing the travel time itself. Because of the variety in individual research on high speed airbreahting propulsion, the information is scattered. Therefore, a European "Long-Term Advanced Propulsion Concepts"-program has been started. The project investigates turbine based- and rocket based combined cycles.

In this project, the Revolutionary Turbine Accelerator, developed by NASA and General Electric Aircraft Engines, will be simulated within the modelling and simulation tool, EcosimPro. This simulation will be limited to the turbomachinery part of the original trajectory of this turbine based combined cycle.

First of all, the supersonic variable cycle augmented turbofan jet engine + ramjet running on kerosene will be classified with respect to the other jet engines and the variable cycle engines. Second, the original engine operation is analysed and simplified to model in EcosimPro. Some new components will be made and validated. After the implementation of the values based on experience, some detailed simulations will be performed to find other unknown parameters. Finally, the total engine model will be simulated and the results compared with literature and practical values.

First, the aft valve effects in the bypass channels are suggested as "0". Next, a two shock conical inlet is chosen and an ideal "Core Driven Fan Stage" is composed. After some tests, it is proven that the best results are obtained with the less dynamic and idealized NASA tables. Therefore, they are used in the next simulations. Instead of the inlet, the "Core Driven Fan Stage" reacted as expected. Initial values were taken from the Pratt & Whitney F100-220E. Next, the possible pressure quotient between the bypass channels is tested and an increasing range with increasing input speed is found. The maximal air flow is limited with the critical value in the afterburner and the pressure quotient between the bypass channels. Then, the fan pressure quotient is determined for the ideal situation at Sea Level Static[1]. Finally, a realistic output is found in which the Take-Off condition is the most demanding phase of flight.

The turbomachinery part of a supersonic engine is simulated in a software tool designed for subsonic engines by creating new components and determining the engine parameters with their physical boundaries and based on experience with the thrust as the only specification. The engine model is also validated with a similar engine in another software program and delivers a realistic output.

[1] Standard aviation conditions for static airplane with an altitude of 0m, temperature of 15 °C and a pressure of 101325Pa.

Abstract (Dutch)

Veel onderzoek en ontwikkeling in de commerciële luchtvaart is in de laatste decennia gewijd aan het reduceren van het brandstofverbruik terwijl de transporttijd zo goed als gelijk bleef. Omdat er al veel, maar individueel onderzoek is gebeurd op het gebied van "high speed airbreathing propulsion" is er een Europees gecoördineerd "Long-Term Advanced Propulsion Concepts and Technologies"-programma opgezet. Dit onderzoekt gecombineerde jet motoren gebaseerd op zowel turbine- als raket technologie.

Hier zal de door NASA en General Electric Aircraft Engines ontwikkelde "Revolutionary Turbine Accelerator" gesimuleerd worden in de "modelling and simulation tool", EcosimPro. De simulatie zal zich beperken tot het turbomachine gedeelte in het origineel vluchttraject voor deze turbine gebaseerde motor.

Eerst wordt deze supersone kerosine turbofan jet engine met naverbranding + ramjet en variabele motorcyclus gesitueerd ten opzichte van de andere jet motoren en de motoren met variabele cyclus. Hierna wordt het origineel werkingsprincipe geanalyseerd en de motorcyclus gesimplificeerd om in EcosimPro te modelleren. Nieuwe componenten worden gemaakt waarna ze volledig getest en gevalideerd worden. Na invoeren van ervaringswaarden worden beperkte simulaties uitgevoerd om de overige onbekende waarden te bepalen. Tot slot wordt het totale model gesimuleerd en resultaten vergeleken met literatuur en praktijk.

Eerst worden klepeffecten in de bypass kanalen als "0" verondersteld. Hierna wordt een "2 shock" conische inlaat verondersteld en een ideale "Core Driven Fan Stage" samengesteld. Na testen bleken de minder dynamische en geïdealiseerde NASA tabellen een beter resultaat op te leveren waardoor ze gebruikt zijn in volgende simulaties. De "Core Driven Fan Stage" reageerde wel zoals voorspeld. Startwaarden werden genomen van de Pratt & Whitney F100-220E. Het mogelijke drukverschil tussen de bypass kanalen werd getest en een stijgende range met stijgende inputsnelheid waargenomen. Vervolgens werd het maximale luchtdebiet gelimiteerd door de kritische snelheid in de naverbrander en drukverschil tussen de bypass kanalen. De fan drukcoëfficiënt vastgelegd op de optimale waarde op "Sea Level Static"[2]. Tot slot werd een realistische output gevonden waarin de Take-Off fase als zwaarste conditie erkend wordt.

Het turbomachine gedeelte van een supersone motor is gesimuleerd in een pakket voorzien voor subsone motoren. Dit door nieuwe componenten te creëren, de motorparameters te bepalen a.d.h.v. fysieke grenzen en ervaringwaarden met enkel de stuwkracht als gegeven. Het motormodel is tevens gestaafd met een model in een andere software en levert een realistische output.

[2] Standaard luchtvaartcondities voor een stilstaand vliegtuig op een hoogte van 0m, temperatuur van 15 °C en een druk van 101325Pa.

Table of Contents

List of Figures

List of Tables

List of Acronyms

AB	AfterBurner
AGARD	Advisory Group for Aeronautical Research and Development
ATF	Advanced Tactical Fighter
BPR	ByPass Ratio
CDFS	Core Driven Fan Stage
CFD	Computational Fluid Dynamics
EL	EcosimPro Language
ESA	European Space Agency
ESTEC	European Space Research and Technology Centre
GEAE	General Electric Aircraft Engines
GESTPAN	GEneral Stationary and Transient Propulsion Analysis
HiMaTE	High Mach Turbine Engine
HiSPA	High-Speed Propulsion Assessment
HP	High Pressure
LAPCAT	Long-Term Advanced Propulsion Concepts and Technologies
LPT	Low Pressure Turbine
NASA	National Aeronautics and Space Administration
NGLT	Next Generation Launch Technology
P&W	Pratt & Whitney
PQ	Pressure Quotient
RBCC	Rocket Based Combined Cycle
RR	Ram Recovery
RTA	Revolutionary Turbine Accelerator
SFC	Specific Fuel Consumption
SLS	Sea Level Static
SPR	Static Pressure Ratio
STA	Service Technique de l'Aéronautique
STOVL	Short Take-Off and Vertical Landing
STR	Static Temperature Ratio
T/W	Thrust to Weight ratio
TBCC	Turbine Based Combined Cycle
TMS	Thermal Management System
TSTO	Two Stage To Orbit

VABI	Variable Area Bypass Injector
VCE	Variable Cycle Engine
VIGV	Variable Inlet Guide Vanes

List of Symbols

η	calculation angle
θ_b	semi spike angle
β	shock angle
ϕ	speed angle relative to the surface of the body
$\vec{V}$	speed vector
A	area
d	inner diameter
D	outer diameter
M	Mach number
p	static pressure
q	velocity
T	static temperature
u	speed parallel to the surface
v	speed perpendicular to the surface
γ	specific heat ratio

Subscripts:

0	state before discrete event
1	state after discrete event
MAX	maximum value
MIN	minimum value
NASA	value from NASA reference
normal	for the normal shock
oblique	for the oblique shock
OP	optimal

1 Introduction

1.1 Background

1.1.1 von Karman Institute

History

It all started in 1922, when the Belgium Ministry of Defence raised a building to house the "Service Technique de l'Aéronautique" (STA) in Sint-Genesius-Rode. The STA was responsible for the certification, testing and inspection of aircrafts, aircraft components and equipment as well as aeronautical ground facilities. Because Belgium was engaged in aircraft design and construction at that time, the building was also designed to accommodate a large low speed wind tunnel. In 1935, some extra laboratories and offices were built. After the war, in 1949, the last building was added to the complex, specially designed to house a supersonic tunnel and a multi-configuration low speed facility. It is worthwhile to mention that in the period between 1930 and 1940 a lot of pioneering work was carried out on helicopters. Under the supervision of scientist Nicolas Florine, the first tandem rotor helicopter using co-rotating rotors was designed.

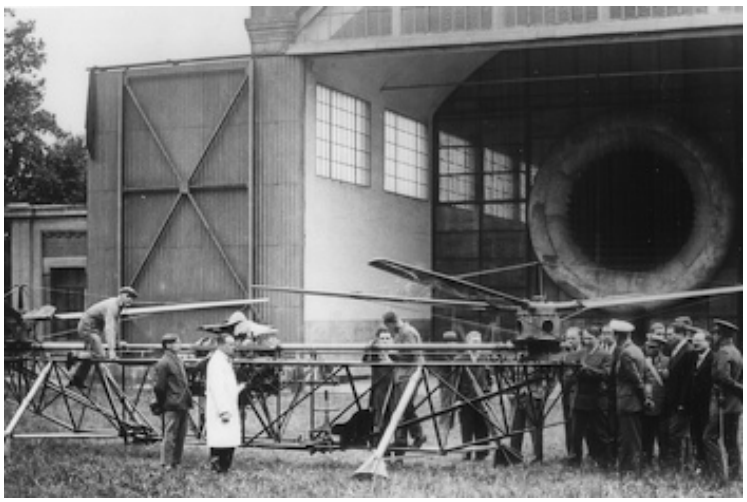

Figure 1.1 Florine II in front of the large low speed tunnel [1]

After WWII, the aircraft inspection, certification and airworthiness part of the STA moved out to Brussels. So only the aerodynamics laboratory left at Sint-Genesius-Rode which was then jointly operated by the Civil Aviation Authority and the national aeronautical research centre. In the course of 1955, Theodore von Karman, who was chairman of the Advisory Group for Aeronautical Research and Development (AGARD), proposed the establishment of an institution devoted to training and research in aerodynamics which would be open to young engineers and scientists of the NATO nations. With the full backing of the Belgian national delegates to AGARD, keeping in mind the existing facilities, the Belgian Government agreed to host the project centre in Sint-Genesius-Rode. After negotiations between Belgium and the USA concerning the practical aspects, the official agreement for the centre was signed in Paris in September 1956 by the Belgian and US government. The Institute was born!

Theodore von Karman acted as the Institute's Chairman between 1956 and his death in 1963. In memory of its founder, the Institute's name was changed in 1963 to the "von Karman Institute".

Figure 1.2 Theodore von Karman [2]

Today, the von Karman Institute is supported by 15 NATO nations, international agencies as well as industries. It houses about 50 different wind tunnels and a large range of turbomachinery and other test facilities.

Structure and research domains

The structure of the von Karman Institute is based on its three research domains: aeronautics & aerospace, environmental & applied fluid dynamics and turbomachinery & propulsion.

The *aeronautics & aerospace* department houses a large range of facilities to test from low speed regime for commercial aircrafts up to supersonic and hypersonic flows of atmospheric space entry. Most of the time however is spent on the modelling, simulation and experimental validation of atmospheric entry flow and thermal protection systems.
The *environmental & applied fluid dynamics* department has a large expertise in the study of aero acoustics, multiphase flows, vehicle aerodynamics, biological flows and environmental flows. Also CFD (Computational Fluid Dynamics) and numeric modelling for the simulation of physical processes are carried out here.
Last but not least, the *turbomachinary & propulsion* department specializes in the aero-thermal aspects of turbomachinery components for aero-engines and industrial gas turbines, space propulsion units, steam turbines and process industry compressors and pumps. Just like the 2 other departments, a lot of computational simulation and analysis has been done on its research domain.

Of course, these 3 departments are supported by general services such as IT, library, administration, … .

1.1.2 The Revolutionary Turbine Accelerator

The Revolutionary Turbine Accelerator (RTA) is an airbreathing jet engine developed by NASA and General Electric Aircraft Engines (GEAE) in frame of the Next Generation Launch Technology (NGLT)-program. The main objective of the NGLT-program is to reduce costs and to improve safety of space access by implementing re-usable hypersonic vehicles and propulsion technologies. Within this project the RTA represents the Turbine Based Combined Cycle (TBCC) engine concept adjacent to the Rocket Based Combined Cycle (RBCC) concept. More specific, the RTA is a supersonic augmented turbofan Variable Cycle Engine (VCE) with a ramjet running on kerosene. The first ground tests with a midscale engine model, the so-called RTA-1, were performed in 2006.

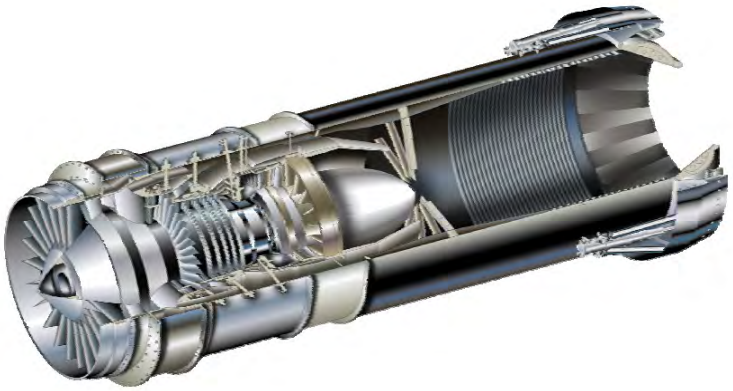

Figure 1.3 Schematic of the RTA-1 [3]

Classification

Before looking further in detail to the RTA and its operation, a small situation sketch is made to form an idea of the relation of the RTA with respect to the other jet engines.

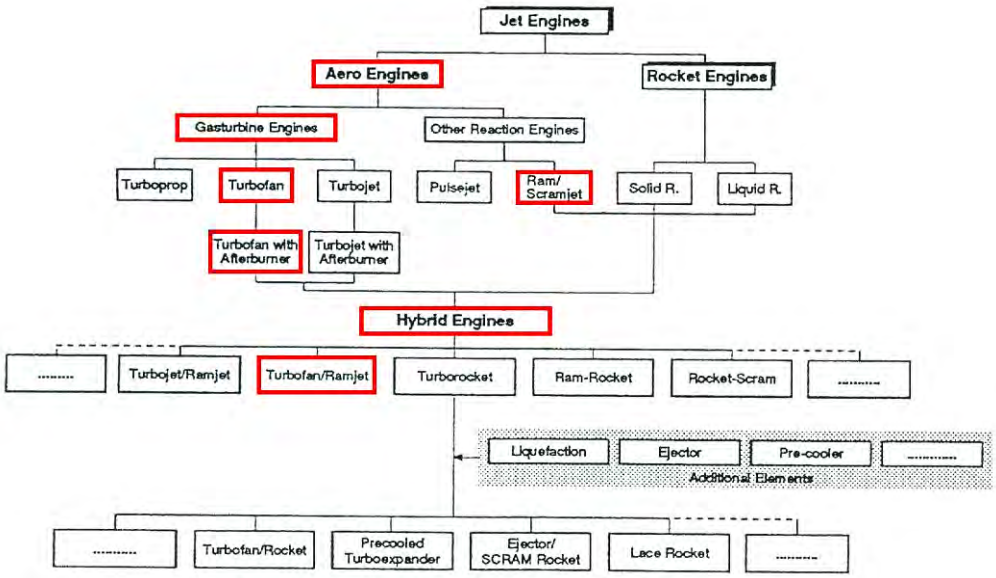

Figure 1.4 Jet engines classification [4]

Like mentioned above, the RTA represents the TBCC engine class so at the first line in figure 1.4 it belongs to the "aero engines"-class.
Second, the core of the engine is an augmented turbofan so the RTA belongs to the "gasturbine engines"-box. It also houses a ramjet, part of the "other reaction engines".
All this leads to a "turbofan/ramjet" in the "hybrid engines"-class.

The last feature of the RTA is that it is a VCE, which means that flow path through the engine can be modified. This kind of system is used to combine the attributes of a high exhaust speed turbojet, i.e., high dry specific thrust[3] and low max power Specific Fuel Consumption (SFC), with those of a high mass flow turbofan, i.e., low part power SFC with low exhaust gas temperature. Furthermore, it creates the possibility to optimize the engine for each point of flight.
A possible classification of these VCE's can be represented like this:

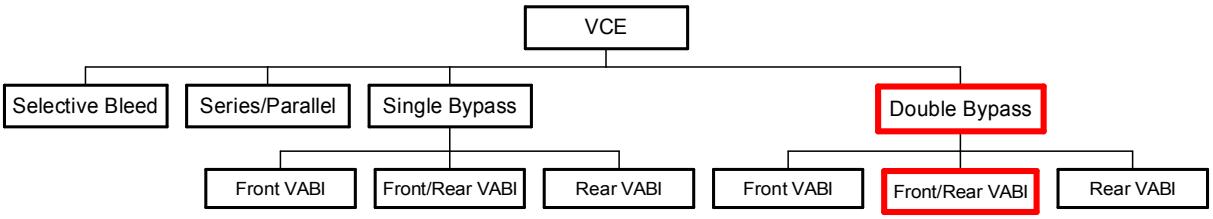

Figure 1.5 VCE classification

In the upper left corner in figure 1.5, the *selective bleed* engine can be found. In this type of engines a part of the flow is bled outside the engine in subsonic mode. They are commonly used in Short Take-Off and Vertical Landing (STVOL)-vehicles. Figure 1.6 shows an example of this type of engine. (High Pressure (HP) valve is open in supersonic mode to avoid overpressure in the HP compressor)
The *series/parallel* engine is a VCE which is capable of placing its bypass tubes in series or in parallel. When they are in parallel, which is shown in the upper part of figure 1.7, a part of the flow from the fans is diverted to the back of the engine and the flow from the inlet tubes into the tip of the Low Pressure Turbine (LPT). This is the low specific thrust mode. When they are in series, in the lower part of figure 1.7, all the flow from the fans stays in the engine but is split between the core engine and the tip of the LPT. This is the high specific thrust mode.
Next are the *single bypass* and *double bypass* engines. The working principle of both types is actually the same. These engines can divert a part of the flow from the low pressure compressor or fans to the back of the engine without passing any turbomachinary. In almost all the cases the flow is dumped just before the AfterBurner (AB). The diverging itself is done by using Variable Area Bypass Injector's (VABI's). These are adjustable valves which can vary the intake area of the bypass channel to control the mass flow and the static pressure. There are a lot of different configurations but they can be split in engines with *front VABI*, *front/rear VABI* and *rear VABI* configuration. The engine from figure 1.8 is very clearly a double bypass engine with a front VABI configuration.
When you compare the different types of VCE's it is obvious that the bypass engines have the most potential to be used with a ram burner. Therefore, the RTA is found in the double bypass with front/rear VABI-class.

---

[3] Thrust divided by the intake mass flow.

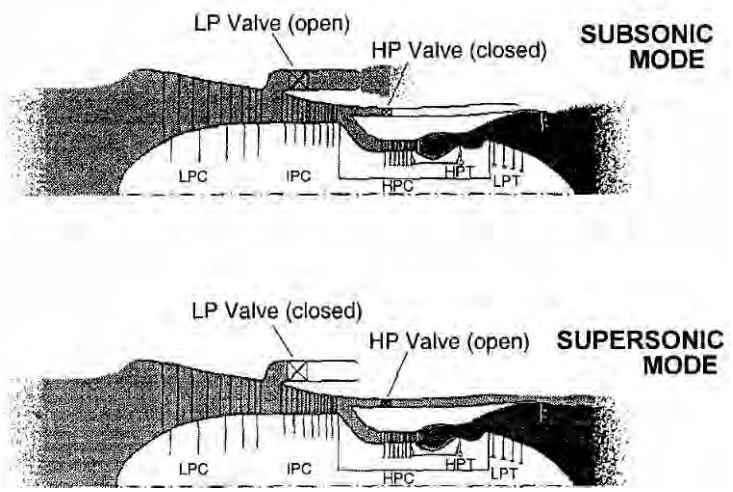

Figure 1.6 Selective bleed engine [5]

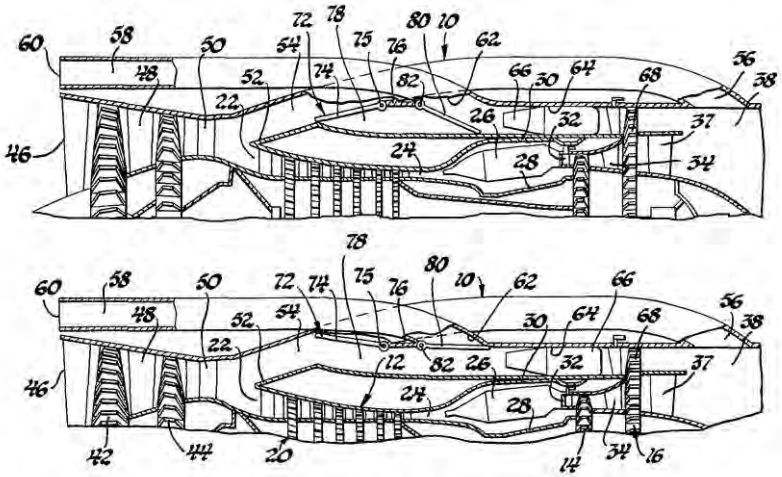

Figure 1.7 Series/parallel engine [6]

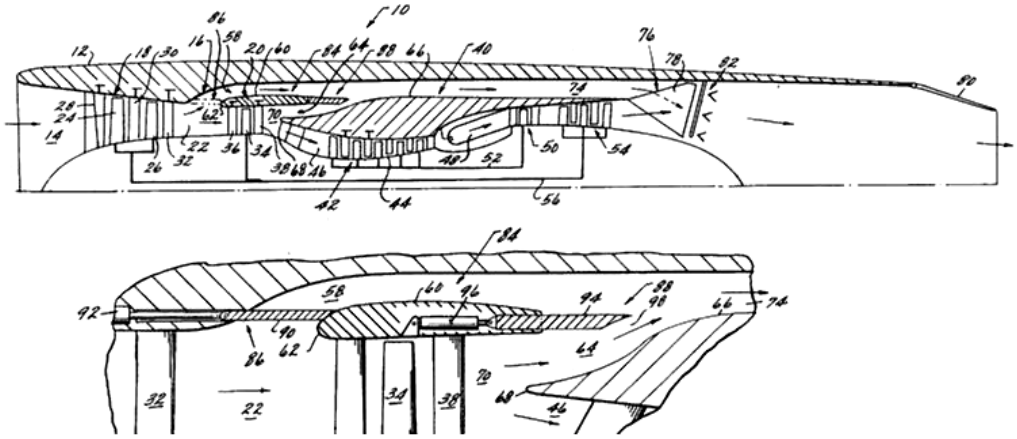

Figure 1.8 Double bypass engine [7]

RTA description

Now it is clear where the RTA is located with respect to the other jet engines, it is time to have a closer, internal look to the RTA itself.

The RTA or GE57 is actually an improved version of the famous Pratt & Whitney (P&W) J58 from the SR-71 or so-called "Blackbird" which made its first flight in 1962. (figure 1.9) Were the J58 ran on endothermic JP7 fuel, used an un cooled circumferential flame holder and a bleed system, the RTA runs on conventional JP8 fuel, uses a cooled radial flame holder and a double bypass configuration. This results in the elimination of some maintenance and durability issues of the J58.

Figure 1.9 Lockheed SR-71 [8]

With this information in the back of our heads, the question "why trying to improve this old engine configuration when there are much more advanced technologies available?" may arise. The answer to this question is given by figure 1.10 and figure 1.11, which is part of the result of the GEAE studies under the US Air Force sponsored High-Speed Propulsion Assessment (HiSPA) and the NASA sponsored High Mach Turbine Engine (HiMaTE) programs between 1986 and 1995.
In figure 1.10 it is obvious that at Sea Level Static (SLS) the turbojets got the largest specific Impulse (I_{sp}) and remain the best up to Mach 5 when followed by a ramjet. This is the reason why a turbo-engine and a ramjet are combined in the TBCC-class. Note that the maximum operating Mach number is already set by choosing this type of propulsion!
The choice for the turbofan/ramjet configuration is determined by the Thrust to Weight ratio (T/W) shown in figure 1.11. Within the NLGT-project, the goal is to reach a T/W of 12 so a turbofan/ramjet configuration clearly has the largest potential! (Today a T/W from 6 to 8 is standard)

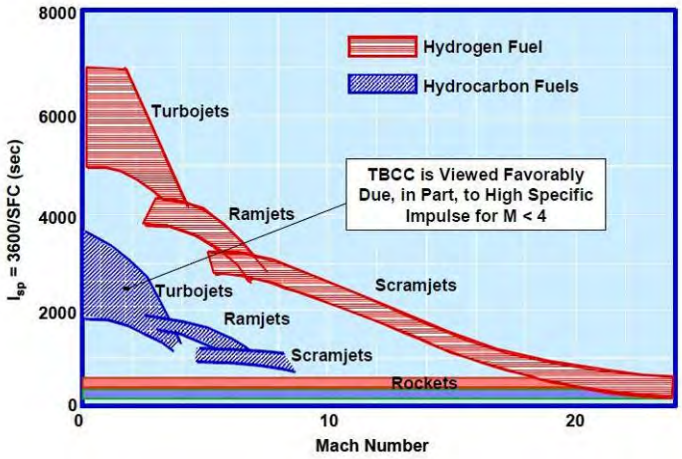

Figure 1.10 Comparison of specific impulse between TBCC and RBCC [9]

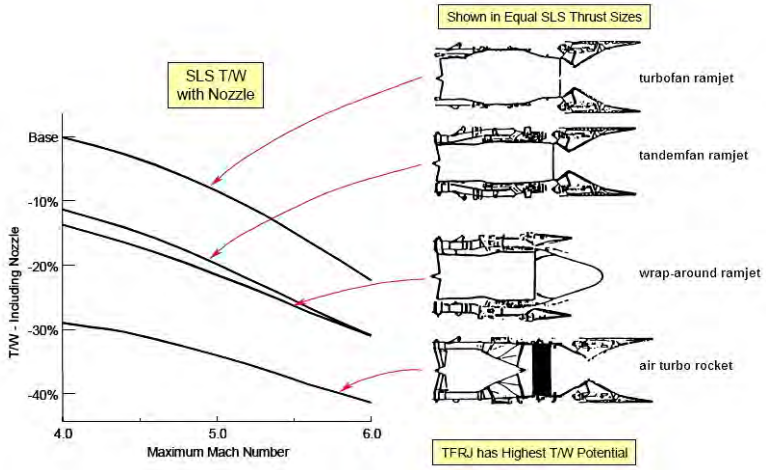

Figure 1.11 Thrust/weight summaries HiSPA [9]

To reduce the engine demonstrator costs, the RTA is based on the GE YF120 (figure 1.12). This engine is a double bypass VCE with a front/rear VABI configuration developed for the US Air force Advanced Tactical Fighter (ATF)-program between 1983 and 1990. GEAE lost this competition against the P&W F119.
To fit the RTA mission profile, some improvements are made (figure 1.13):

- new fan and fan frame;
- new Core Driven Fan Stage (CDFS);
- material upgrades of compressor stage 2,3;
- new rear VABI system;
- new hyperburner and slave exhaust;
- sophisticated fuel and Thermal Management System (TMS).

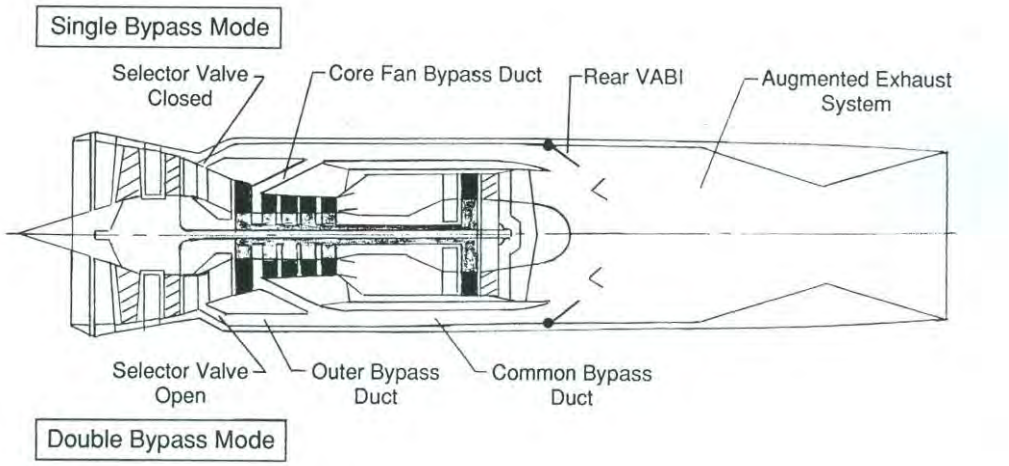

Figure 1.12 GE YF120 [10]

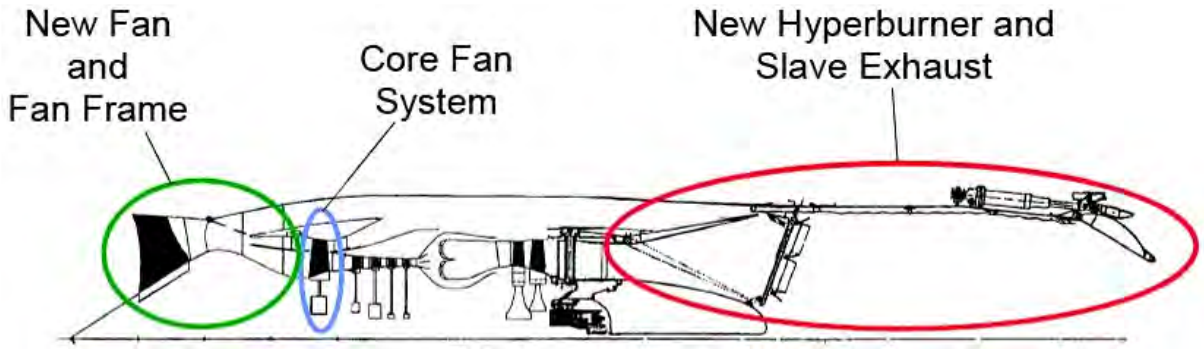

Figure 1.13 Schematic cross section RTA-1 [9]

The *new fan and fan frame* are necessary because the RTA will reach a higher ByPass Ratio (BPR) than the YF120 and the fan has to be aerodynamically invisible when the engine is windmilling. (See "RTA operation" paragraph)
As can be seen in figure 1.12, the YF120 was already equipped with a *CDFS* to reduce the engine diameter. But in the RTA a CDFS is fit with a separation (108) between the tip (107) and hub (109) of the fan, clearly shown in figure 1.14. Using a fan with a separated tip and hub in combination with Variable Inlet Guide Vanes (VIGV) (88 and 90) enables the possibility to change the flow path of the fan apart form each other.
The *material upgrade of compressor stage 2,3* is a logic result of the high Mach mission profile and resulting temperatures of the RTA.
A larger *rear VABI system* reduces mixing losses by a smoother transition in flow state.
The standard augmenter is replaced by a so-called *hyperburner* with a new flame holder and fuel injection system. More detailed information about the hyperburner can be found in reference [11]. Also a new convergent *slave exhaust* system is fitted instead of the convergent-divergent nozzle.
Last a *sophisticated fuel and TMS* is used to withstand the thermal loads during the trajectory and to ensure a smooth mode transition, explained in the next paragraph.

A schematic figure like 1.13 has to be interpreted with care: these figures are made to hide details! A related patent like figure 1.14 shows much more information about the practical implementation than a schematic one.

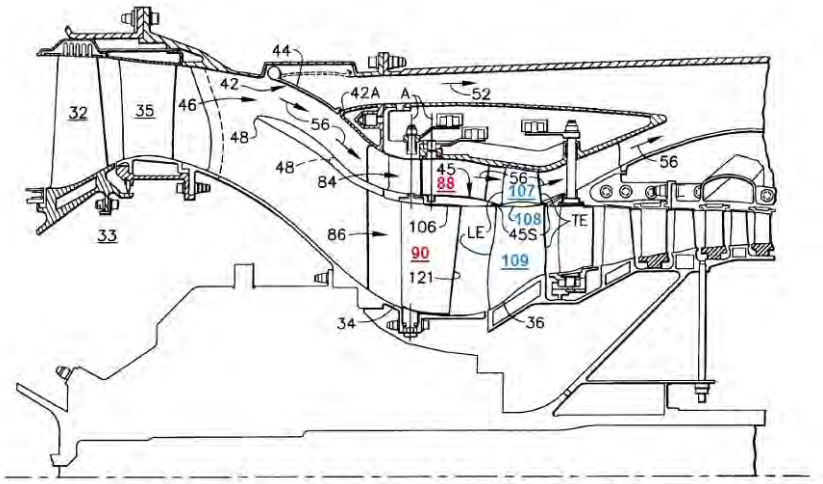

Figure 1.14 Cross sectional view front configuration [12]

RTA operation

Next the RTA operation conditions will be explained, and illustrated by figure 1.15, in function of the flight speed. Each flight speed also represents a certain altitude which can be found in the trajectory (figure 1.16).

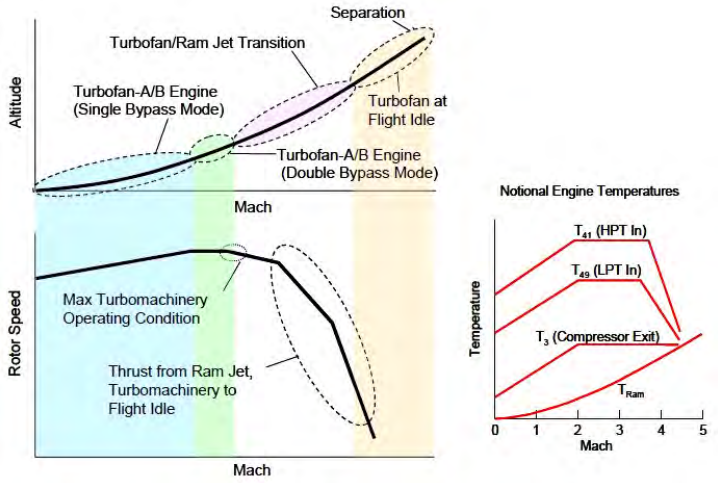

Figure 1.15 RTA-1 operation and operating temperatures [13]

SLS ≤ M ≤ 1,6

From Take-Off until Mach 1,6, the RTA acts like a normal single bypass augmented turbofan engine. This means the first VABI is fully closed and most of the air delivered to the hyperburner comes from the core stream. Meanwhile the rotor speed accelerates and temperatures rise through the supersonic shocks and increasing engine load. At Take-Off the engine must deliver more than 150.000N (35.000 lb) of thrust.

$2 < M \leq 3$

At Mach 2, the engine starts the transition to ramjet mode. The core engine is still running but the fuel flow to the core is decreasing while the flow to the hyperburner is increasing. Also the fan pressure ratios will decrease between Mach 2 and 3 which is mainly a result from the decreasing fuel flow, and resulting rotor speeds, but also from the position of the VIGV. Within this Mach range, the front VABI also reaches its maximum opening position!

$3 < M \leq 3{,}5$

Between Mach 3 and 3,5, the rotor speeds as well as the turbine temperatures diminish. At Mach 3,5 the engine is completely windmilling which is necessary to ensure a quick engine restart, to drive the accessory equipment and to reduce the mechanical loads on the rotating components when they are exposed to the highest inlet temperatures which will increase engine life.

$M > 3{,}5$

The engine is completely operating in ramjet mode and when $M > 4$ the Two Stage To Orbit (TSTO) launch vehicle will separate.

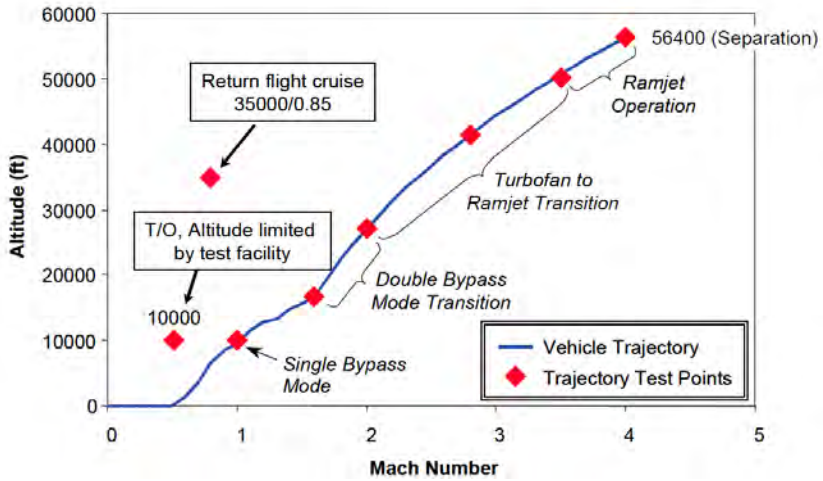

Figure 1.16 TSTO trajectory [9]

When the trajectory is completed the engine will be brought back to subsonic flight speeds and will fly back to base.
During the total trajectory a 10x swing in BPR is reached between core and bypass stream!

1.2 Project description

1.2.1 Motivation

In the last decades a lot of research is spent on aircraft configurations and related propulsion engines to reduce the SFC without changing the propulsion techniques to reduce the travel time itself.
Because a lot of individual research on high-speed airbreathing propulsion has been done by different institutions, the information is scattered. To prevent this, the European Commission has launched a 3 year LAPCAT-project, LAPCAT being an acronym for "Long-Term Advanced Propulsion Concepts and Technologies", and started in 2005. The program is a corporation between 4 industries, 4 research centres and 4 universities coordinated by ESA-ESTEC and has as main goal to reduce the travel time of long-distance flights. It ended in April 2008 and was followed by 4 year LAPCATII-project which started in October 2008. This latter is in frame of the first one, focussing on the RTA based concepts in the TBCC-category adjacent to the also investigated RBCC's.
Using a modelling and simulation tool to investigate an engine is a low-cost method to evaluate the engine configurations and chances to fit the requested mission profile. Pressure ratio's, different fuel types, blade geometries, … can be adapted and tested within minutes!

More information about LAPCAT can be found in reference [14].

1.2.2 Objective

The objective of this project is to model and simulate a RTA engine model, as correct as possible, in the modelling and simulation software, EcosimPro. In frame of the LAPCATII-project.
To limit the project space, the engine model and working principle of the RTA-1 is used and performed on base of the standard TURBOJET-library. Beginning from a very simplified model and refining it as much as possible in the available time period.
The simulations will be based on the RTA's TSTO-trajectory and will be limited in first phase to the turbomachinary part.

2 Modelling

2.1 EcosimPro: modelling and simulation tool

The modelling and simulation tool EcosimPro has been chosen to execute the simulations. Some other programs which can be used for gas turbine simulations are Gasturb [15] and GSP [16] but have more restrictions.

EcosimPro is designed to be a user-friendly modelling and simulation tool developed by "Empresarios Agrupados International", a Spanish architect-engineering company. It can be used to model physical processes that can be expressed in terms of differential-algebraic equations or ordinary differential equations and discrete events.

The modelling of physical components is based on the EcosimPro Language (EL) which is an object-oriented modelling language. This is one of the big advantages of EcosimPro. The user can concentrate on the physical meaning of his equations and not on how to implement them to be useful for computer simulations. For example, EcosimPro will internally rearrange an equation to find an equality for its unknown variable or implementing a derivative by using a simple hyphen.

The modelling itself is done by linking distinct icons, which represent components, to each other. Those components are always based on global constants & variables, functions and ports.
The concepts *global constants & variables* speak for themselves. They are constants or variables which are used for the global model or in each separate component. For example: gravity, standard atmosphere, altitude, Mach number, chemical elements, … .
Functions are used to calculate the thermodynamic properties of the gasses and fluids. They consist of tables with thermodynamic coefficients, control functions and the functions to calculate the properties itself.
The *ports* are used to link the different components to each other. In a port the behaviour is defined by variables and equations depending on its type. For example in a force port, the output force is the sum of the input forces.
When different components are linked with ports, this combination becomes a component itself which can be used to make more complex systems. In this way EcosimPro employs a set of basic and advanced libraries containing various types of components (mechanical, electrical, pneumatic, turbojet, …) that can be used to model a lot of different types of systems.

Once a code is written or a schematic is made, the EL file must be compiled. The compiling is necessary to convert the EL code into a code useful for computer simulation. This process is executed by a C++ compiler.

Now the code is compiled, the user needs to define a partition which represents the mathematical model of the component. There are 3 options: a default- , a user defined- and a design partition. In each partition the user needs to define a certain amount of boundaries, necessary to obtain a unique solution for the mathematical model. These need to be chosen very carefully since they stay constant during all the experiments based on this partition.

To solve a box of equations, the boundaries need to be assisted by so called “algebraic variables” which are actually initial values.
A design partition contains one extra kind of variable that has to be selected: the design variables. These variables are initialised with a default value and need to be designed depending on the specific system.

Now a partition has been created it is possible to run an infinite amount of experiments based on one partition. In this experiment the bounds and algebraic variables need to be initialised to calculate steady states or to integrate the model with respect to the time.

Below, the specific EcosimPro modelling terminology is written in a different size and font and is not added to the symbols- or acronyms list. For more specific information, consult general references [24], [25] or the TURBOJET-library.

2.2 Functions

Here the functions which are added to the standard TURBOJET-library are described.

Because the engine is working in the supersonic domain, a supersonic inlet is necessary. In a supersonic inlet there will be shocks which are not described in EcosimPro. Therefore it is necessary to write shock functions. There are 3 shock situations: a normal shock, an oblique shock and an oblique followed by a normal shock. The implementation of these 3 cases is described below.

In each function the Ratio of the Static Pressure p (SPR) and Temperature T (STR) are calculated and the aft shock Mach number (M_1). The total ratios and density ratio will not be calculated since the standard EcosimPro functions can perform these calculations based on the static ratios.
Each of the following equations suggests conservation of mass, energy and momentum. Also the viscous effects are ignored.
The condition before the shock uses index 0, the aft shock condition index 1.

2.2.1 Normal shock

The following equations are used:

$$\frac{p_1}{p_0} = \frac{2\gamma M_0 - (\gamma - 1)}{\gamma + 1} \tag{2.1}$$

$$\frac{T_1}{T_0} = \frac{\left[2\gamma M_0^{\,2} - (\gamma - 1)\right]\left[(\gamma - 1)M_0^{\,2} + 2\right]}{(\gamma + 1)^2 M_0^{\,2}} \tag{2.2}$$

$$M_1 = \sqrt{\frac{(\gamma-1)M_0^{\,2}+2}{2\gamma M_0^{\,2}-(\gamma-1)}} \qquad \textbf{(2.3)}$$

Where:

- γ specific heat ratio.

Implemented in an EcosimPro code file:

```
FUNCTION NO_TYPE  normal_shock(
        IN REAL gamma,
        IN REAL Mach0,
        OUT REAL SPR,
        OUT REAL STR,
        OUT REAL Mach1
)

BODY
        SPR = ((2*gamma*Mach0**2 - (gamma - 1)) / (gamma + 1))
        STR = ((2*gamma*Mach0**2 - (gamma-1))*((gamma - 1)*Mach0**2 + 2))/((gamma + 1)**2*Mach0**2)
        Mach1 = sqrt(((gamma - 1)*Mach0**2 + 2)/(2*gamma*Mach0**2 - (gamma - 1)))

END FUNCTION
```

2.2.2 Oblique shock past a cone

Like shown in the figure 2.1, the oblique shock is calculated around a cone. The β-angle is the difficult part of the calculation. There is no problem computing β for a 2D profile but when you are using a cone, a 3D conical shock will be created. In that case, it is necessary to work with circular coordinates. But an easier way of computation can be found in reference [17].

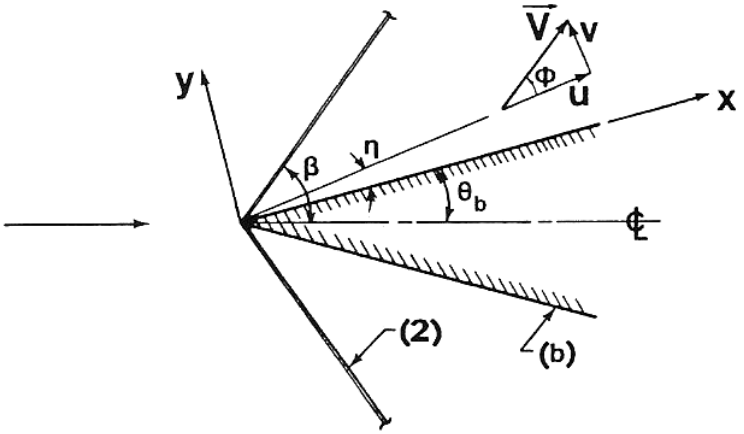

Figure 2.1 Oblique shock past a cone [17]

Where:

- β shock angle (rad);
- η calculation angle (rad);
- θ_b semi spike angle (°);
- $\vec{V}$ speed vector (m/s);
- ϕ speed angle relative to the surface of the body (rad);
- u speed parallel to the surface (m/s);
- v speed perpendicular to the surface (m/s).

Based on homentropic relations[4], p and q represents the pressure and velocity respectively.

$$p = \left\{ \frac{1 + [(\gamma - 1)/2] M_b^2}{1 + [(\gamma - 1)/2] M_\eta^2} \right\}^{\gamma/(\gamma - 1)} \tag{2.4}$$

$$q = \frac{M_\eta}{M_b} \left\{ \frac{1 + [(\gamma - 1)/2] M_b^2}{1 + [(\gamma - 1)/2] M_\eta^2} \right\}^{1/2} \tag{2.5}$$

$$\frac{d\phi}{d\eta} = \frac{\sin(\phi + \theta_b)}{\sin(\eta + \theta_b)} \frac{\cos(\phi - \eta)}{M_\eta^2 \sin(\phi - \eta)^2 - 1} \tag{2.6}$$

$$\frac{dM_\eta}{d\eta} = \frac{\sin(\phi + \theta_b)}{\sin(\eta + \theta_b)} \frac{M_\eta \{1 + [(\gamma - 1)/2] M_\eta^2\} \sin(\phi - \eta)}{M_\eta^2 \sin(\phi - \eta)^2 - 1} \tag{2.7}$$

M_η and M_b represents the aft shock Mach number at the calculated angle and the body surface respectively.

$$\frac{[M_\eta^2 \sin(\phi - \eta)^2 - 1] \sin(\eta + \theta_b)}{\{1 + [(\gamma - 1)/2] M_\eta^2 . \sin(\phi - \eta)^2\} \sin(\phi + \theta_b)} \cos(\phi - \eta) + 1 = 0 \tag{2.8}$$

When the equation 2.8 is satisfied, the shock angle is reached which means:

$$\eta_1 = \eta \qquad M_1 = M_\eta \qquad \theta_1 = \varphi + \theta_b \qquad \beta = \eta + \theta_b$$

$$M_0 = \left[\sin(\beta)^2 - \frac{\gamma + 1}{2} \frac{\sin\theta_1 \sin\beta}{\cos(\theta_2 - \beta)} \right]^{-1/2} \tag{2.9}$$

---

[4] Fluid flow in which the entropy per unit mass is the same at all locations in the fluid and at all times.

For the integration itself, a fourth order Runge-Kutta method is used. Mainly because the standard integration process in EcosimPro is to slow for dynamic calculations.
Below the integration method for the M_η is shown, but is analogue for ϕ. With "i" the integration step.

$$M_{\eta(i+1)} = M_{\eta i} + \frac{step}{6}(m_1 + 2m_2 + 2m_3 + m_4) \tag{2.10}$$

$$m_1 = \frac{dM_{\eta i}}{d\eta_i} \tag{2.11}$$

$$m_2 = \frac{dM_{\eta(i+\frac{step}{2}m_1)}}{d\eta_{(i+\frac{step}{2})}} \tag{2.12}$$

$$m_3 = \frac{dM_{\eta(i+\frac{step}{2}m_2)}}{d\eta_{(i+\frac{step}{2})}} \tag{2.13}$$

$$m_4 = \frac{dM_{\eta(i+step.m_3)}}{d\eta_{i+step}} \tag{2.14}$$

Finally, the SPR and STR can be calculated. For the STR, the isentropic relation is used since the M_0 and M_1 are known. For the SPR, the equation for the 2D oblique shock can be used because β is calculated for the 3D problem.

$$\frac{p_1}{p_0} = \frac{2\gamma M_0^2 \sin(\beta)^2 - (\gamma - 1)}{(\gamma + 1)} \tag{2.15}$$

$$\frac{T_1}{T_0} = \frac{\left[1 + \left(\frac{\gamma - 1}{2}\right)M_0^2\right]}{\left[1 + \left(\frac{\gamma - 1}{2}\right)M_1^2\right]} \tag{2.16}$$

Below, the EcosimPro code file:

```
FUNCTION NO_TYPE  oblique_shock(
        IN REAL gamma,
        IN REAL theta_b,
        IN REAL Mach0,
        OUT REAL Mach1,
        OUT REAL SPR,
        OUT REAL STR
)
```

```
DECLS
        REAL Mach[1000]
        REAL phi[1000]
        REAL p[1000]
        REAL q[1000]
        REAL test[1000]
        REAL step = 0.001

        REAL m1_mach
        REAL m2_mach
        REAL m3_mach
        REAL m4_mach

        REAL Mach_2
        REAL Mach_3
        REAL Mach_4

        REAL m1_phi
        REAL m2_phi
        REAL m3_phi
        REAL m4_phi

        REAL phi_2
        REAL phi_3
        REAL phi_4

        REAL eta[1000]
        INTEGER i
        BOOLEAN flag = TRUE

        REAL beta
        REAL Mach0_integ
        REAL Mach_b
        REAL phi_shock

BODY
        Mach_b = 1

        WHILE (Mach0_integ < Mach0)

        flag = TRUE

        FOR (i IN 1,1000)
                Mach[i] = 0
                phi[i]  = 0
                eta[i] = 0
                test[i] = 0
        END FOR

        Mach[1] = Mach_b
        i = 1

        WHILE (flag == TRUE)
                p[i] = ((1 + ((gamma - 1)/2)*Mach_b**2)/(1 + ((gamma - 1)/2)*Mach[i]**2))**(gamma/(gamma - 1))
                q[i] = (Mach[i]/Mach_b)*((1 + ((gamma - 1)/2)*Mach_b**2)/(1 + ((gamma - 1)/2)*Mach[i]**2))**(0.5)
                test[i] = ((Mach[i]**2 * (sin(phi[i] - eta[i]))**2 ) - 1) * sin(eta[i] + theta_b) * cos (phi[i] - eta[i]) / ((1 + ((gamma -
                1)/2)*Mach[i]**2 * sin(phi[i] - eta[i])**2)*sin(phi[i] + theta_b)) + 1

                IF (test[i] > 0) THEN
                        flag = FALSE
                        phi_shock = theta_b + phi[i-1]
                        beta = theta_b + eta[i-1]
                        Mach1 = Mach[i-1]
                        Mach0_integ = ( sin(beta)**2 - ((gamma + 1) * sin(phi_shock) * sin(beta))/(2 * cos(phi_shock -
                        beta)))**(-0.5)
                END IF

                eta[i+1] = eta[i] + step
```

```
        m1_mach =  (sin(phi[i] + theta_b)/sin(eta[i] + theta_b))* (Mach[i] * (1 + ((gamma - 1)/2)*Mach[i]**2) * sin (phi[i] -
        eta[i]))/((Mach[i]**2 * (sin(phi[i] - eta[i]))**2) - 1)
        m2_mach =  (sin(phi[i] + theta_b)/sin((eta[i+1] - 0.5*step) + theta_b))* (Mach_2 * (1 + ((gamma -
        1)/2)*Mach_2**2) * sin  (phi[i] - (eta[i+1]-0.5*step)))/((Mach_2**2 * (sin(phi[i] - (eta[i+1] - 0.5*step)))**2) - 1)
        m3_mach =  (sin(phi[i] + theta_b)/sin((eta[i+1] - 0.5*step) + theta_b))* (Mach_3 * (1 + ((gamma -
        1)/2)*Mach_3**2) * sin  (phi[i] - (eta[i+1]-0.5*step)))/((Mach_3**2 * (sin(phi[i] - (eta[i+1]-0.5*step)))**2) - 1)
        m4_mach =  (sin(phi[i] + theta_b)/sin(eta[i+1] + theta_b))* (Mach_4 * (1 + ((gamma-1)/2)*Mach_4**2) * sin
        (phi[i] -  eta[i+1]))/((Mach_4**2 * (sin(phi[i] - eta[i+1]))**2) - 1)
        Mach_2 = Mach[i] +  (1/2) * step * m1_mach
        Mach_3 = Mach[i] +  (1/2) * step * m2_mach
        Mach_4 = Mach[i] +  step * m3_mach

        m1_phi = (sin(phi[i] + theta_b)/sin(eta[i] + theta_b)) * cos (phi[i] - eta[i])/((Mach[i]**2 * sin(phi[i] - eta[i])**2) - 1)
        m2_phi = (sin(phi_2 + theta_b)/sin((eta[i+1] - 0.5*step) + theta_b)) * cos (phi_2 - (eta[i+1]-
        0.5*step))/((Mach[i]**2 *  sin(phi_2 - (eta[i+1]-0.5*step))**2) - 1)
        m3_phi = (sin(phi_3 + theta_b)/sin((eta[i+1] - 0.5*step) + theta_b)) * cos (phi_3 - (eta[i+1] -
        0.5*step))/((Mach[i]**2 *  sin(phi_3 - (eta[i+1]-0.5*step))**2) - 1)
        m4_phi = (sin(phi_4 + theta_b)/sin(eta[i+1] + theta_b)) * cos (phi_4 - eta[i+1])/((Mach[i]**2 * sin(phi_4 -
        eta[i+1])**2) - 1)

        phi_2 = phi[i] + 0.5 * step * m1_phi
        phi_3 = phi[i] + 0.5 * step * m2_phi
        phi_4 = phi[i] + step * m3_phi

        phi[i+1] = phi[i] + (1/6) * step * (m1_phi + 2*m2_phi + 2*m3_phi + m4_phi)
        Mach[i+1] = Mach[i] + (1/6) * step * (m1_mach + 2*m2_mach + 2*m3_mach + m4_mach)

        i += 1

    END WHILE

    Mach_b = Mach_b + step

    END WHILE

    SPR = (2*gamma * (Mach0_integ**2) * (sin(beta)**2) - (gamma - 1))/(gamma + 1)
    STR = (1 + (gamma-1)*0.5*Mach0**2)/(1 + (gamma-1)*0.5*Mach1**2)

END FUNCTION
```

2.2.3 Conical inlet shocks

As already mentioned, the shock functions are written to make a supersonic inlet. In particular, a conical inlet.
Before writing these functions some suggestions are made:

- 2 shock inlet: an oblique followed by a normal shock;
- cone always in proper position: oblique shock at inlet edge (no spillage);
- zero angle of attack;
- no cone compression: normal shock at $M_0 = 1$ and $M_{1\ oblique} = M_{0\ normal}$.

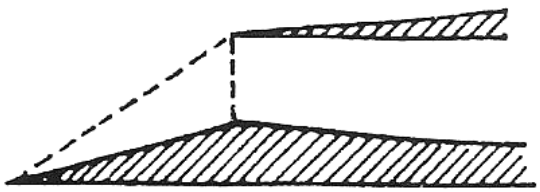

Figure 2.2 Two shock conical inlet [18]

The minimum M_0 for a completely supersonic conical flow field in function of θ_b can be found in reference [19]. With these values a polynomial is calculated with a correlation factor of 0,9997.

$$M_{0\min} = 0{,}0005\theta_b^2 + 0{,}0063\theta_b + 1 \quad \textbf{(2.17)}$$

When M_0 is lower than $M_{0\,min}$, only a normal shock will take place. But for some reasons the oblique shock can also be started above mach 2 because:

- there is no reference data available below Mach 2;
- the design calculations can be performed with normal shock calculations which are much faster.

Starting at $M_{0\,min}$, logically gives a smoother transition in SPR and STR. Below, the oblique shock function is starting at $M_{0\,min}$.

The EL-code file:

```
FUNCTION NO_TYPE oblique_normal_shock(
        IN REAL gamma,
        IN REAL theta_b,
        IN REAL Mach0,
        OUT REAL SPR,
        OUT REAL STR,
        OUT REAL Mach1
)

DECLS
        REAL Mach0_min
        REAL theta
        REAL SPRo
        REAL STRo
        REAL Mach1o
        REAL SPRn
        REAL STRn
        REAL TTRn

BODY
        Mach0_min = 0.0005 * theta_b**2 + 0.0063 * theta_b + 1
        IF(Mach0 > 1) THEN
        --IF(Mach0 >= 2)THEN
        IF(Mach0 >= Mach0_min)THEN
                theta = theta_b * PI/180
                oblique_shock(gamma, theta, Mach0, SPRo, STRo, Mach1o)
                IF(Mach1o > 1)THEN
                        normal_shock(gamma, Mach1o, SPRn, STRn, Mach1)
                        SPR = SPRo * SPRn
                        STR = STRo * STRn
                END IF
        ELSE
                normal_shock(gamma, Mach0, SPRn, STRn, Mach1)
                SPR = SPRn
                STR = STRn
        END IF
        ELSE
        SPR = 1
        STR = 1
        Mach1 = Mach0
        END IF

END FUNCTION
```

2.3 Ports and global constants & variables

Non of the ports or global constants & variables were adapted.

2.4 Components

Almost every component keeps its standard value. The inlet is the only element that is adapted by the shock function described in paragraph 2.2.3 . The modifications are briefly described below. Furthermore, a new component is created, the CDFS. The layout and source code modifications are explained as well.

2.4.1 Conical inlet

Mentioned in paragraph 2.2, only the SPR, STR and M_1 are used to calculate the conditions at the inlet. The total values will be processed by the standard EcosimPro functions.
The modifications are described for each type of variable.

PORTS
/

DATA
Added:

```
REAL theta      "semi spike angle (°)"
```

DECLS
Added:

```
REAL SPR
REAL STR
REAL Mach1
REAL Ts1
REAL k1
```

CONTINUOUS
modified parts

```
--calculation environmental conditions
Ts1 = Tamb + dTamb
Psat = psat_H2O(Ts1)
k1 = Cp_T_FAR(Ts1, g_out.FAR) / (Cp_T_FAR(Ts1, g_out.FAR) - R_FAR(g_out.FAR))

oblique_normal_shock(k, theta, Mach, SPR, STR, Mach1)

--converting environmental to aft shock condition
Ts = Ts1 * STR
k= Cp_T_FAR(Ts, g_out.FAR) / (Cp_T_FAR(Ts, g_out.FAR) - R_FAR(g_out.FAR))
v = Mach1 * sqrt(k * R_FAR(g_out.FAR) * Ts)
Pt_in = (SPR*Pamb) * exp((Phi_T_FAR(g_out.T, g_out.FAR) –
Phi_T_FAR(Tamb*STR, g_out.FAR)) / R_FAR(g_out.FAR))
```

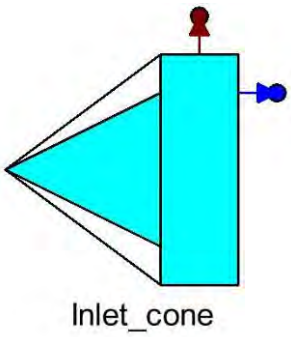

Figure 2.3 Inlet cone

2.4.2 Core Driven Fan Stage

As explained in chapter 1, the RTA is equipped with a CDFS.

Because simply multiplying the output pressure of the fan bypass stream will not affect the fan work, a completely new component is created to be able to work with a different Pressure Quotient (PQ) for hub and tip. This component consists of 2 compressors, a split fraction, 1 input & 2 output gas ports and an input & output shaft port.

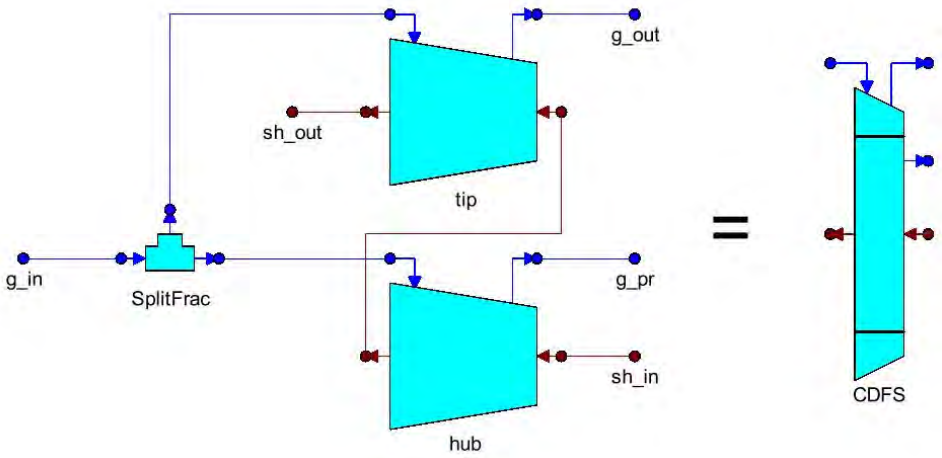

Figure 2.4 CDFS

Notice that the shafts of the hub- and tip compressor are placed in series. The result is the same for parallel, but we need one more boundary condition. Because now EcosimPro know for sure the 2 compressors are on the same axis.

After compiling this component, some small modifications to the source code are made.
First the code is adapted so the maps and default design rotation speed for the hub and tip compressor are the same. Also the default correction factors for the maps are made editable in the CDFS component.
Second the branch factor of the split fraction is changed. This value determines the BPR of the CDFS.

Last, an extra continuous block is made to ensure the input hub- and tip pressure is equal. This is necessary because the branch pressure is not defined in the standard SplitFrac-component code.
Modified parts of the code:

```
DATA
        REAL ND_CDFS = 10000
        REAL l_tip = 10
        REAL l_hub = 10
        REAL CG1_tip = 1
        REAL CG2_tip = 1
        REAL CG4_tip = 1
        REAL CG1_hub = 1
        REAL CG2_hub = 1
        REAL CG4_hub = 1

        TABLE_2D F1_CDFS
        TABLE_2D F2_CDFS
        TABLE_2D F3_CDFS

DECLS
        ALG REAL BPR          "Bypass Ratio (-)"

TOPOLOGY
        TURBOJET.Compressor tip(
                l = l_tip,                  -- Non default value.
                ND = ND_CDFS,               -- Non default value.
                CG1 = CG1_tip,              -- Non default value.
                CG2 = CG2_tip,              -- Non default value.
                CG4 = CG4_tip,              -- Non default value.
                F1 = F1_CDFS,               -- Non default value.
                F2 = F2_CDFS,               -- Non default value.
                F3 = F3_CDFS                -- Non default value.
        )

        TURBOJET.Compressor hub(
                l = l_hub,                  -- Non default value.
                ND = ND_CDFS,               -- Non default value.
                CG1 = CG1_hub,              -- Non default value.
                CG2 = CG2_hub,              -- Non default value.
                CG4 = CG4_hub,              -- Non default value.
                F1 = F1_CDFS,               -- Non default value.
                F2 = F2_CDFS,               -- Non default value.
                F3 = F3_CDFS                -- Non default value.
        )

        TURBOJET.SplitFrac SplitFrac(
                k = BPR / (1 + BPR)     -- Non default value.
        )

CONTINUOUS
        tip.g_in.P = hub.g_in.P
```

Note that the scalar for primary flow compression work and efficiency, repetitively DH- and EPD ratio, which are used in the standard fan component, are not implemented by using compressors instead of fans.

2.5 RTA engine model

Now every necessary component is made, the complete RTA engine model can be assembled.

Intake

There is no intake defined for the RTA-1, so the inlet cone, made in paragraph 2.4.1, is used. Every suggestion made during the composition of this component remains valid.

Fans

The first fan is modelled as a standard EcosimPro fan. The second fan is the CDFS made in paragraph 2.4.2.
For the maps, F1, F2 and F3 from the examples in the TURBOJET_EXAMPLES-library are used. This is not completely correct, but because the real blade profile is unknown this is apt enough to run the first basic simulations.

VABI's

For the first simulations the two VABI's are replaced by ordinary mixers because in the first phase the max duct area has to be determined before aft valve effects can be implemented.

Turbines

The standard EcosimPro turbines are used. Using the turbine maps, G1 and G2, from the examples in the TURBOJET_EXAMPLES-library.

For all the other components, the standard components are used. Like all the other components, they use their default initial values.

The total RTA engine model, which is used in the rest of the text, is shown in figure 2.5.

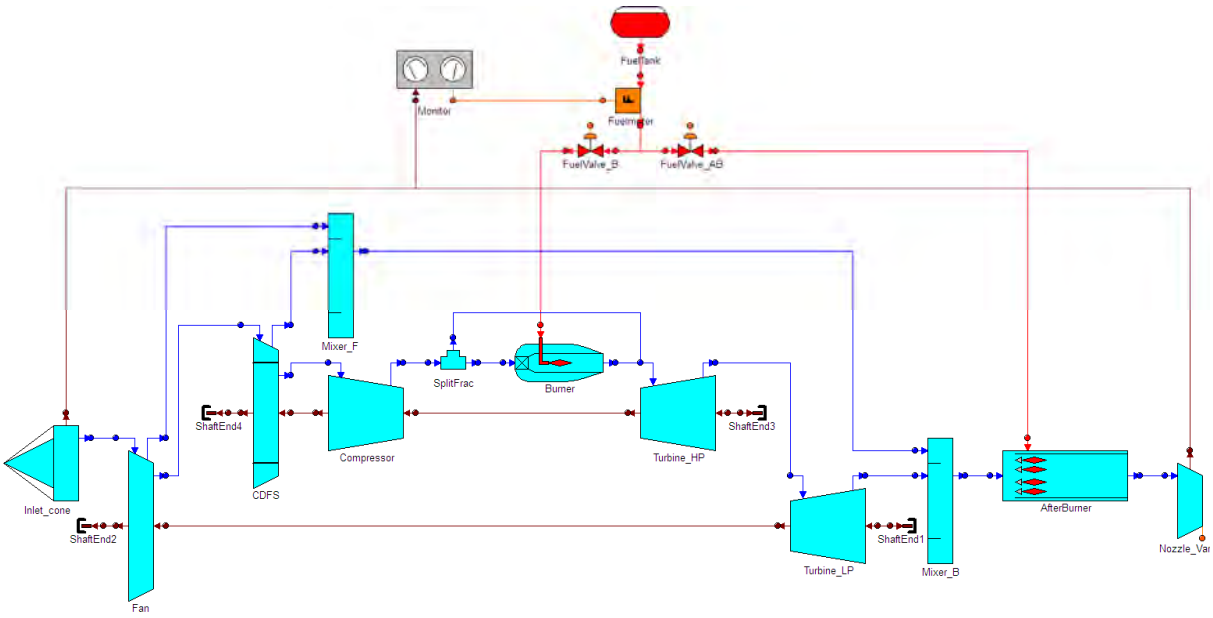

Figure 2.5 RTA engine model

3 Simulation

When the engine model is ready and compiled without errors, it is possible switch to a next stage in the project: the simulation.

Before the actual simulations of the total engine model, a mathematical model of the engine needs to be created identical to the description in paragraph 2.1. More particular it needs to be a design partition, because every other simulation is based upon these results.
After realistic figures for the initial values and boundaries are selected, the self-made functions and components are tested. These components are already compiled but the CDFS need a larger assembly to be tested. Of course, the total model is tested as well for a realistic output.
Before the total engine model is simulated along its trajectory, some detailed simulations of critical components are performed.

3.1 Design partition

The name "design partition" speaks for itself: it will design the engine components. This design partition, which is nothing more than a mathematical model, is created with 3 different wizards. The design-, boundaries- and algebraics wizard. These three selected variables are discussed below.

3.1.1 Design wizard

Within this wizard, the design variables are selected. These variables are found in the DATA-block of each component.

Turbomachinery

For the compressors and fans, the correction factors CG1, CG2 and CG4 and also CG3 for the turbines are selected. These factors are necessary to perform the map-scaling.
An extra variable, the design rotational speed ND, is chosen for 1 component/shaft to calculate the actual rotation speed.
The inertial moment "I" is left on its default value: 10kg/m². It only becomes important in transient partitions which can be integrated with respect to the time.

Mixers

Both cross sectional areas, A1 and A2, are selected. They need to be designed to know the maximum cross sectional area necessary for future aft valve effects.

Burner

The chamber volume (VOL) and loss coefficient (GLP) are the only DATA-variables of which it makes sense to choose them, because CX is a set of coefficients.

AB

For the AB, the cross sectional area A is selected because the other two variables already use realistic default values.

Nozzle

The nozzle exit area A_exit is the only DATA-variable in the component.

The other components, shown on the right side of figure 3.1, only contain variables with realistic default values and are un-necessary to be chosen.

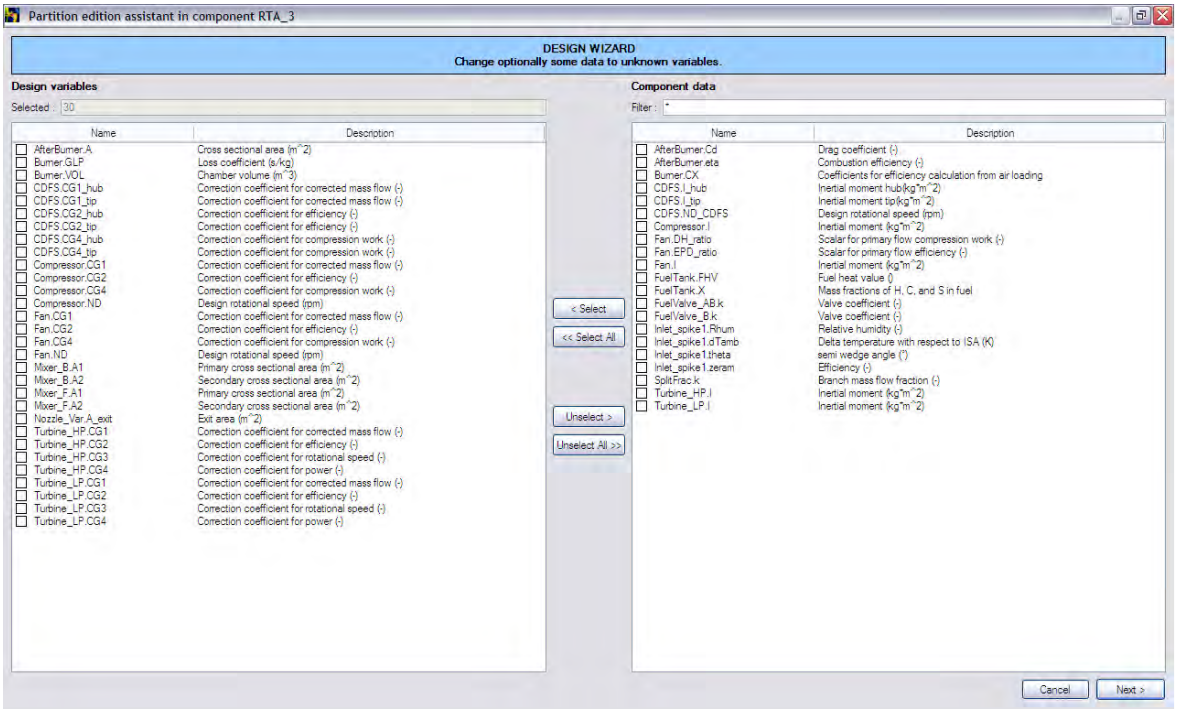

Figure 3.1 Design wizard

3.1.2 Boundaries wizard

Because most of the components contain more variables than equations, some boundary-variables need to be chosen to solve the equations. The boundaries and their values have to be determined very precisely because almost all of them stay constant in all the simulations based on the output of a certain design partition.
The entire model needs 35 boundaries.

Fans

For a fan the BPR, PQ, efficiency EPD and β are selected.
When the ND is chosen in the design partition, also the derivative of the rotational speed DN and a dimensional rotational speed PCNR are added to the list.

Compressor

A compressor is the same as a fan but the BPR and PQ are replaced by input mass flow g_in.W and output pressure g_out.P.

Mixers

Instead of static pressure Ps, standard selected in the TUROJET-examples, the primary flow Mach number M1 is chosen. The reason for this will become clear in paragraph 3.4.2.

Burner

Just like what is done in all the examples, the air loading AL and PQ are selected.

Turbines

For both turbines the non scaled power DHQTJ, EPD and non scaled corrected rotational speed NRJ is chosen.

The HP turbine gets an additional boundary g_in.T to limit the turbine input temperature.

AB

The input Mach number M_in is a very critical parameter for the AB.

Nozzle

To limit the heat added by the entire cycle, g_in.T is chosen besides of the area signal A.signal. The area signal is time dependant and can be changed, apart from the other boundaries, in a next part of the simulations.

Global

The global variables, TURBOJET.Altitude and TURBOJET.Mach, are automatically added to the list.

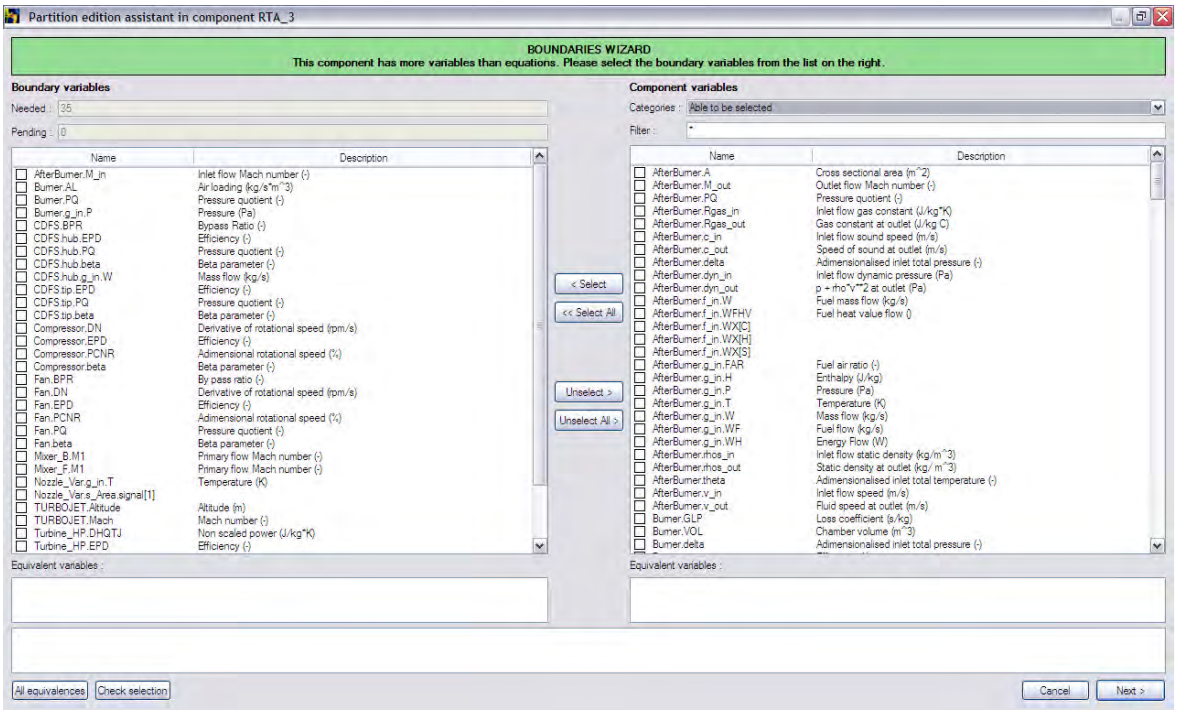

Figure 3.2 Boundaries wizard

Notice that some of the input or output boundaries are defined in terms of an input or output of a subsequent or previous component. These equivalences can be checked by clicking the button “All equivalences” or are displayed in the “equivalent variables” dialog box when selected.

3.1.3 Algebraics wizard

Last the design partition contains an additional wizard, the algebraics wizard.
Within these wizard some extra variables needs to be chosen to solve a so-called box, which is a set of non linear algebraic equations. These variables are used as an initial condition to start solving the equations within on an iterative way.

The following variables are chosen to solve 5 boxes:

- Mixer_F.Ts1 (static temperature channel 1);
- Turbine_HP.g_in.W;
- Mixer_B.Ts1;
- AfterBurner.A;
- AfterBurner.f_in.W (AB fuel flow).

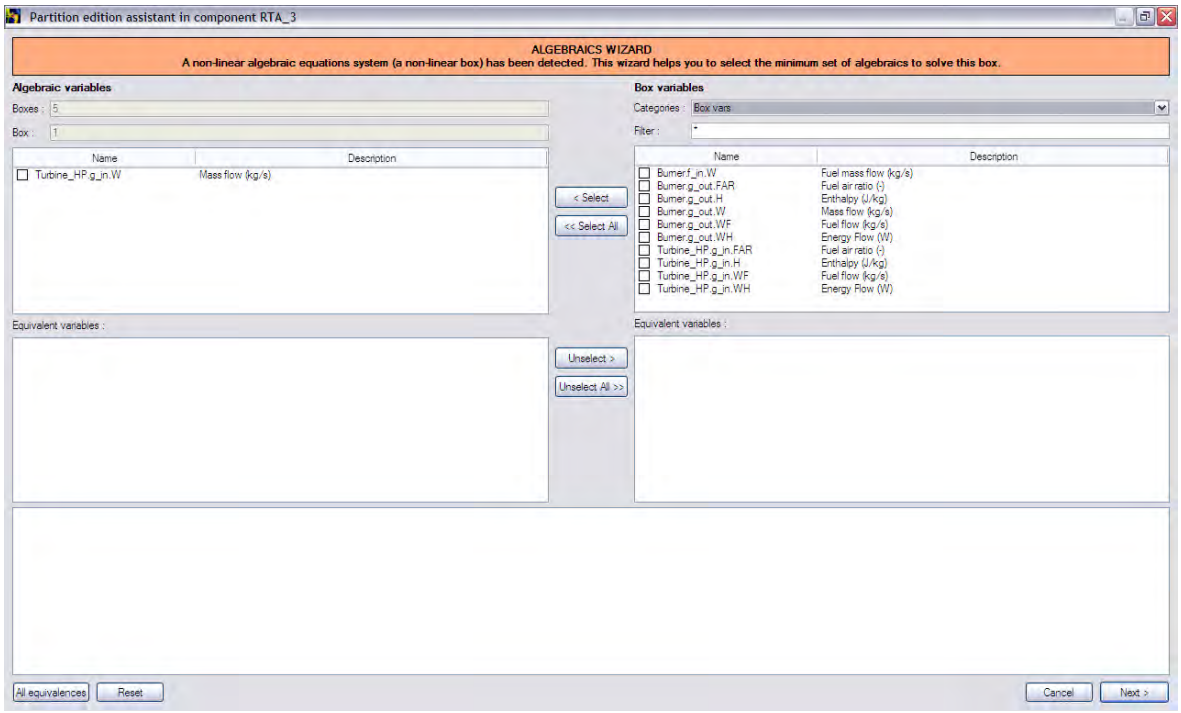

Figure 3.3 Algebraics wizard

3.2 Input values

The last step before simulations can be started is giving realistic values to the initial- and boundary variables.
These values are based upon the TUBOJET_EXAMPLES, data from similar jet engines and are confirmed by reference [20].

The initial values:

```
-- State variables
Compressor.N = 13000
Fan.N = 11500

-- Algebraic variables
Mixer_F.g_in1.T = 300
Mixer_F.g_in2.T = 300
Mixer_F.Ps1 = 1e+5
Mixer_F.Ts1 = 200
Compressor.g_in.T = 300
SplitFrac.g_in.T = 500
Turbine_HP.g_in.W = 60
Mixer_B.Ps1 = 1e+5
Mixer_B.Ts1 = 200
AfterBurner.A = 0.3
AfterBurner.f_in.W = 1
```

The boundaries:

```
--fixed
.EPD = 0.92
.beta = 0.7
.PCNR = 92
.DN = 0
.DHQTJ = 1
.NRJ = 1
Mixer_F.M1 = 0.7
Burner.AL = 2.5
Burner.g_in.P = 25e+5
Burner.PQ = 0.96
Turbine_HP.g_in.T = 1800
Mixer_B.M1 = 0.3
AfterBurner.M_in = 0.3
Nozzle_Var.g_in.T = 2000
Nozzle_Var.s_Area.signal[1] = 1

--temporary unknown
TURBOJET.Altitude
TURBOJET.Mach
Fan.BPR
Fan.PQ
CDFS.BPR
CDFS.hub.g_in.W
CDFS.hub.PQ
CDFS.tip.PQ
```

3.3 Validation

Before simulating the total model, it has to be checked the functions, components and the entire engine model are working correctly. This way, an overload of errors in the total model can be avoided.

3.3.1 Oblique shock past a cone

To make sure the oblique shock is giving a correct output, the values for the STR, SPR and M_0 are compared with reference [19] for a given input γ and θ_b.

Input:

- γ 1,4;
- θ_b 20°;
- integration step 0,001.

M_0	2	3	4	5	6	7	8	10
STR	1,1450310	1,3146023	1,5278297	1,7894001	2,1085664	2,4584823	2,8856263	3,8487118
STR_{NASA}	1,1441172	1,3085950	1,5195513	1,7777106	2,0856763	2,4452172	2,8573859	3,8418751
Dev. (%)	0,08	0,46	0,54	0,66	1,10	0,54	0,99	0,18
SPR	1,5895324	2,3992092	3,5599180	5,0546183	6,8451701	9,1628234	11,6327607	18,5702392
SPR_{NASA}	1,5860610	2,3974074	3,5458514	5,0203638	6,8198807	8,9446745	11,3950720	17,2736630
Dev. (%)	0,22	0,08	0,40	0,68	0,37	2,44	2,09	7,51
M_1	1,6911681	2,3768906	2,9571925	3,4300722	3,8005908	4,1188312	4,3487493	4,7203661
$M_{1\ NASA}$	1,6930228	2,3871521	2,9698263	3,4461044	3,8285609	4,1332695	4,3758337	4,7255026
Dev. (%)	-0,11	-0,43	-0,43	-0,47	-0,73	-0,35	-0,62	-0,11

Table 3.1 Oblique shock results

As shown in table 3.1, the maximum deviation (dev.) is 7,51 % (SPR) when M_0 = 10. Since M_0 is limited to 4,5 for the RTA, the maximum deviation stays below 0,68 % (SPR) which is an acceptable value.
As seen, the largest differences are found with the SPR. These are caused by the use of the 2D equation. For higher Mach numbers, a more accurate way of calculation is recommended.
Reducing the integration step will have an overall improvement but also a large influence on the calculation time.

3.3.2 Conical inlet

The oblique shock function is tested in the previous paragraph and the normal shock function uses exact equations. This means, the conical inlet can be tested on the following statements:

Across a shockwave:

- SPR > 1;
- STR > 1;
- Total Temperature Ratio (TTR) = 1;
- total enthalpy = constant;
- Total Pressure Ratio (TPR) < 1.

The first two statements are a classic result of the abrupt gas property changes over a shockwave. The TTR and total enthalpy stay constant because a shockwave does no work and there is no heat addition. Last, the decreasing TPR is a result of the non-isentropic character of a shockwave.

To perform the test itself, a normal inlet is compared with the conical inlet. The normal intake delivers the reference output without shocks and the conical inlet with the effect of the shocks. The following bounds are used:

- altitude 0m;
- Mach 0 – 4,5;
- g_in.W 300kg/s;
- θ_b 20°.

And the following values are compared:

- STR Ts;
- TTR Tt_in;
- total enthalpy g_out.H;
- TPR Pt_in.

As seen in paragraph 2.4.1 the inlet conditions of the standard inlet are re-written to the aft shock conditions in the conical inlet and can be used to prove the statements on top of this page.
Notice that there is no output value for the SPR, but based on 3.1.1 the statement for the SPR is fulfilled.

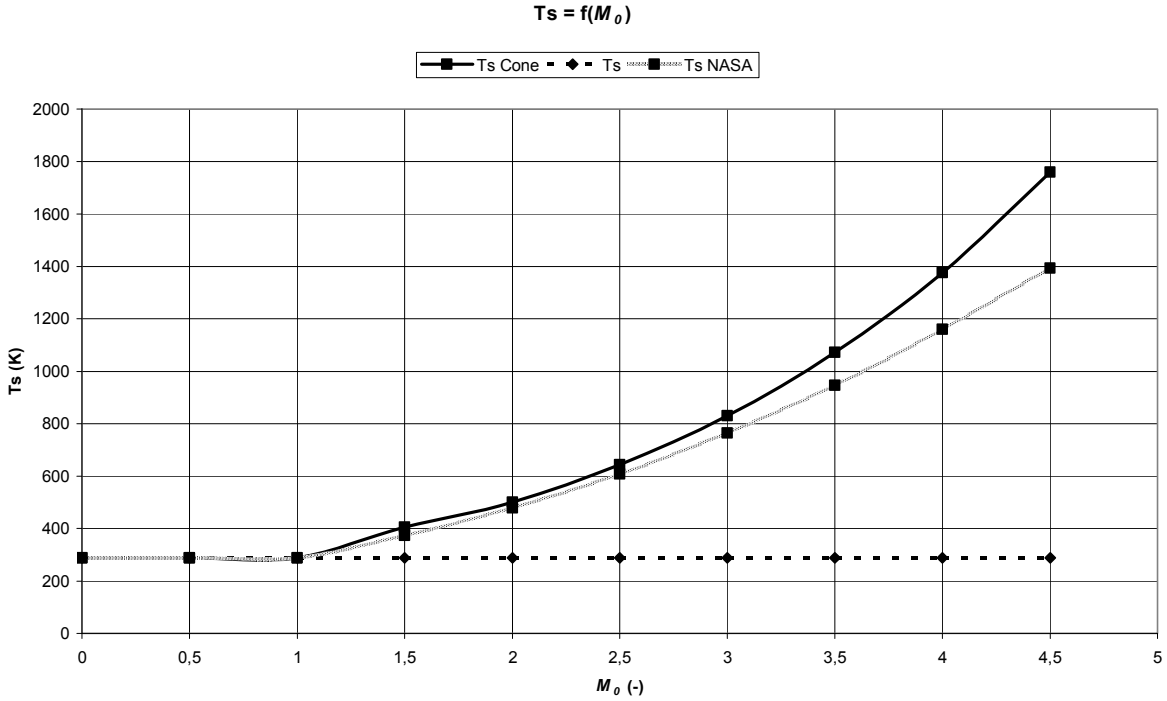

Figure 3.4 Normal vs. conical inlet: Ts

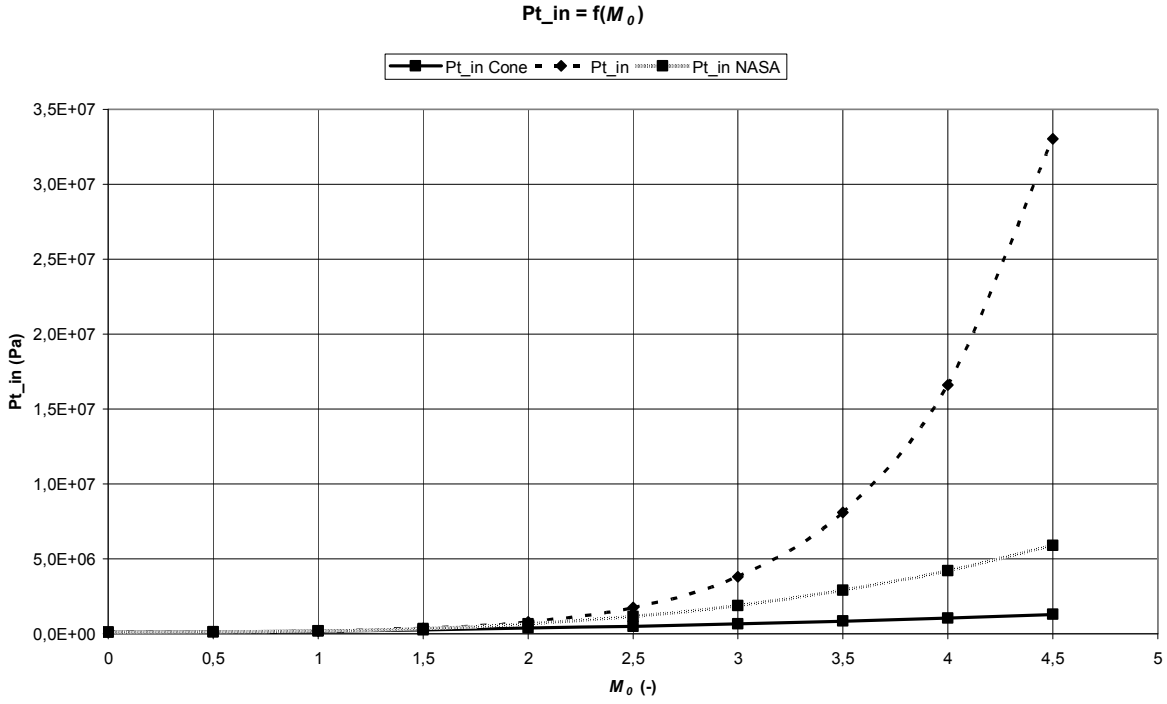

Figure 3.5 Normal vs. conical inlet: Pt_in

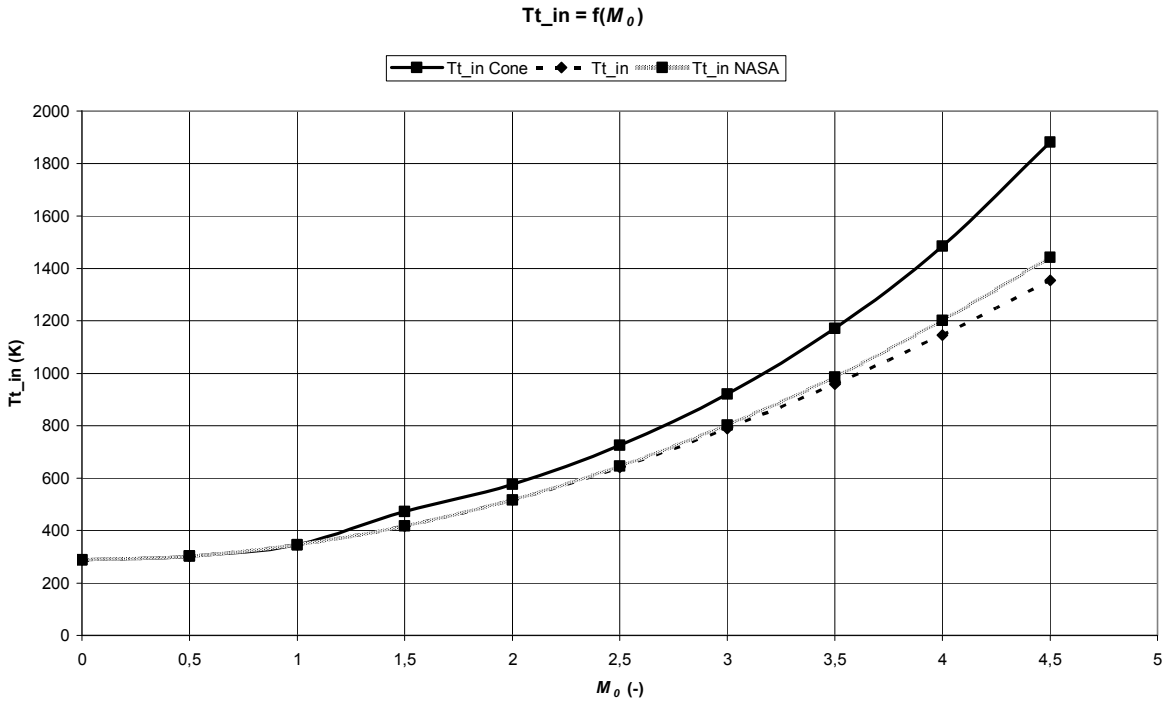

Figure 3.6 Normal vs. conical inlet: Tt_in

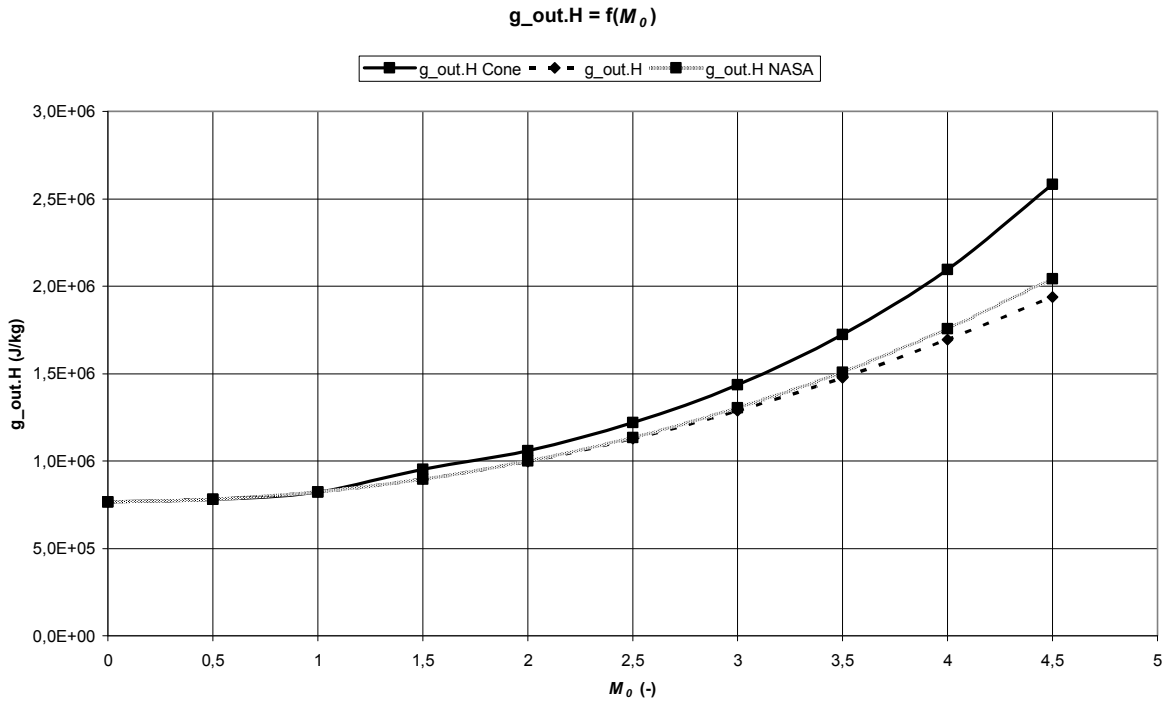

Figure 3.7 Normal vs. conical inlet: g_out.H

In figure 3.4, the increase in static temperature is very obvious. Furthermore, the decrease in static pressure can be seen in figure 3.5.
Normally, figure 3.6 and 3.7 should show a clear overlay since the TTR and total enthalpy stay constant. Because there are small deviations on the STR, SPR and M_1 which increase with increasing M_0 and all the other properties are however calculated on base of these 3, larger deviations are found for the TTR and total enthalpy. To be sure if these large errors are caused by these small deviations, also an inlet is written were the oblique shock function is replaced by the NASA reference tables. Each table gives the STR, SPR or M_1 respectively for a certain M_0.

The trend of both results is identical but the deviation of those with the NASA tables is much smaller. The tables are less dynamic since they use a standard γ of 1,4 and are only valid for one θ_b. The latter, θ_b is never changed and γ will not differ that much from 1,4. Therefore the tables are used for the following simulations. The oblique shock function itself can still be used in a latter stage of the project, for example to investigate the influence of the semi spike angle.
Notice that there is no standard output variable to control the results for the TPR and STR. But the results of the TTR and total enthalpy are almost the same for those with or without shocks, just like required. Therefore the TPR and STR are assumed as correct.

3.3.3 CDFS

To check if the CDFS is functioning well, the total engine model is used since there are a lot of input and output parameters. The total model is not validated yet but if the design parameters of all the other components stay constant for the same input, the CDFS is valid.
Remember, the CDFS does not use the DH- and EPD ratio so these values are set to 1 for the normal fan.

Showing the results of this control simulation makes no sense since everything is exactly the same except:

- replaced fan correction factors;
- compressor correction factors;
- design rotational speed.

The source of this difference is the default inertial moment. The axis will rotate slower because there is a larger inertial moment for the CDFS. Because the map scaling factors and design rotational speed are less important since the output is the same, “I” is left on its default value.

3.3.4 Engine model

Correctly validating the total engine model is not a simple mission. Suggestions are made concerning the components, default maps are used, … .

A similar augmented double bypass VCE model is calculated in reference [21] with GESTPAN. The engine has no VIGV, no nozzle, some boundaries are unknown and the model does not use maps but is useful to get a general idea of the correctness of the results.
Besides, the idea of switching from Ps to M1 for the mixer boundaries is based on this reference.

Parameter	Value
TURBOJET.Altitude (m)	0
TURBOJET.Mach	0
Fan.BPR	0,3
Fan.EPD	0,88
Fan.g_in.W (kg/s)	100
Fan.ND (rpm)	9000
Fan.PQ	5,0
CDFS.BPR	0,3
CDFS.EPD	0,88
CDFS.PQ	1,37
Mixer_F.M1	0,70
Compressor.ND (rpm)	18000
Compressor.EPD	0,88
Compressor.PQ	4,0
Burner efficiency	0,99*
Burner PQ	0,95*
Turbine_HP.g_in.T (K)	1800
Turbine_HP PQ	2,00*
Turbine_HP.EPD	0,90
Turbine_LP.EPD	0,9
Turbine_LP PQ	2,50*
Mixer_B.M1	0,30
AfterBurner PQ	0,95*

Table 3.2 GESTPAN boundaries [21]

The boundaries used in the GESTPAN model are translated to EL and given, with their appropriate name for the RTA engine model, in table 3.2. The boundaries used in the GESTPAN model which are not used in the RTA engine model are written with an *. The output of both simulations is compared in table 3.3.

Most of the values are in the same order. Only the front mixer areas and the AB area are up to twice as big as the others and this is possibly caused by the modelling differences described above. It uses a compressor instead of a fan as well.

Tool	GESTPAN	EcosimPro
Fan.WR (kg/s)	100,0000	100,9488
Fan.g_out.P (Pa)	506625,0	501558,8
Mixer_F.A1 (m²)	0,127477	0,020966
Mixer_F.A2 (m²)	0,016290	0,028400
Compressor.WR (kg/s)	11,679546	15,349708
Compressor.g_out.P (Pa)	2776305,0	2740000,0
Burner.f_in.W (kg/s)	1,86261	1,76303
Turbine_HP.g_out.P (Pa)	1174171,0	971487,1
Turbine_LP.g_out.P (Pa)	492281,96	411807,25
Mixer_B.A1 (m²)	0,2370055	0,2715429
Mixer_B.A2 (m²)	0,0765053	0,0508306
AfterBurner.A (m²)	0,1769239	0,3805498

Table 3.3 GESTPAN vs. EcosimPro

3.4 Simulations

Finally, the actual simulations of the RTA engine model can be started.

These simulations are based on the TSTO-trajectory, as already mentioned in 1.2.2, and thus will determine the TURBOJET.Altitude and TURBOJET.Mach.
After some initial simulations, the mixers are identified as some of the most critical components and therefore investigated separately. Also the mass flow and the fan PQ need some further investigations to prevent problems and determining the unknowns in paragraph 3.2.
Last the total model is simulated and the results for SLS and the maximum operating condition are compared with each other and the practical values of the P&W F100-220E.

3.4.1 Trajectory

The TSTO-trajectory is already shown in figure 1.16.
The first 3 NASA trajectory test points are used for the simulations including a SLS and Mach 2,6 test point. Since this chart is given in feet, instead of metres, and some values need to be interpolated, a new rough trajectory is made (figure 3.8).

The 5 test points with their altitude and Mach number are given in table 3.4.

Point	1	2	3	4	5
Altitude (m)	0	3048	5029	8230	10790
Mach	0,0	1,0	1,6	2,0	2,6

Table 3.4 Simulation test points

The fifth test point only serves to calculate the maximum bypass area since the maximum operating condition is at Mach 2.

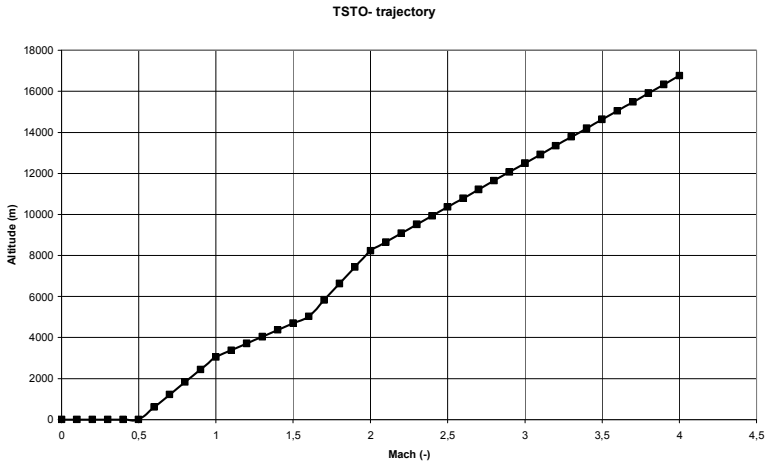

Figure 3.8 Simulation trajectory

3.4.2 Mixers

The main problem with the mixers are backflows. One of both input flows which is pushing the other back to its source. This is caused by the pressure difference between these two flows.
To prevent backflows in the simulations, the possible PQ range between both input channels is investigated for a value of the input Mach number of channel 1 (M1).

First a new design partition for a single mixer is created with the following variables:

- design variables A1, A2;
- boundaries M1, g_in.FAR, .P, .T, .W;
- algebraics Ts1.

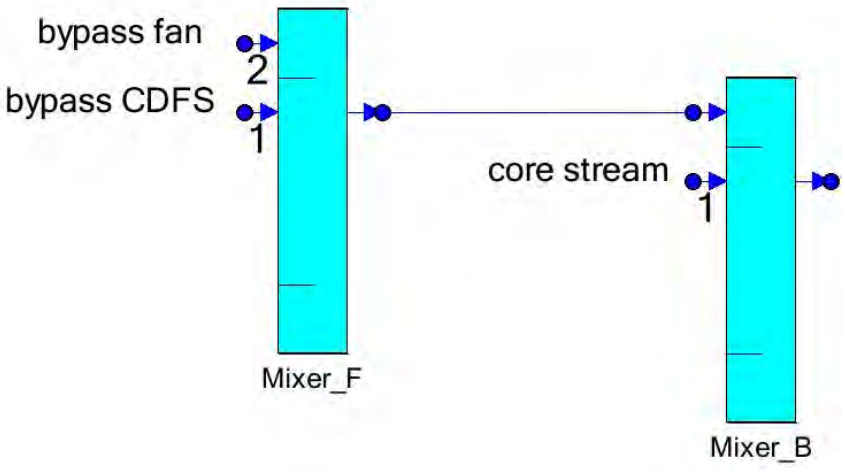

Figure 3.9 Mixer configuration

Notice M1 is chosen as a boundary instead of Ps. Selecting M1 has advantages for the mixer itself but for the relation between both as well. It ensures that there is no backflow in channel 1 since the value is set to a fixed positive number. Next, the matching static pressure between channel 1 and 2 is automatically calculated since al the parameters are known. Also the static pressure in the front mixer is automatically set to a higher value than for the back mixer to reach the fixed input Mach number in both mixers. In this way there will be no backflow from the back- to the front mixer. Figure 3.9 can help to understand the mixer interaction.

Second, the initial values are adapted:

```
Mixer1.Ts1 = 100
Mixer1.Ps1 = 1e+5
```

For the bounds:

- M1 0,1 – 1;
- FAR 0 (Fuel to Air Ratio);
- P fixed for channel 2 and investigated for channel 1;
- T suggested isentropic with $\gamma = 1{,}4$;
- W higher mass flow in channel 2.

The actual value for g_in2.P, T, W and the difference in mass flow have no effect on the results. Only the cross sectional areas will increase with an increasing W and vice versa.
The results of this simulation are shown in table 3.5.

M1	0,1	0,2	0,3	0,4	0,5	0,6	0,7	0,8	0,9	1,0
PQ_{MIN}	0,54	0,55	0,57	0,59	0,63	0,68	0,74	0,81	0,90	1,01
PQ_{MAX}	1,00	1,02	1,06	1,11	1,18	1,27	1,38	1,52	1,68	1,89

Table 3.5 PQ in function of M1

As seen above, with increasing M1, the possible PQ range increases. Also the values of PQ itself increase. Explaining this phenomenon based on the mathematical model of the mixer will outrun the goal of the simulation.

With these results the unknown CDFS hub and tip PQ are limited when M1 of the mixer is defined.

3.4.3 Mass flow

Increasing the mass flow only increases the size of a non-augmented jet engine. But when an AB is used, this mass flow will be restricted. When to much fresh air passes to the AB, to much fuel will be burned and the exhaust Mach number will exceed the critical value 1. All this is based on the assumption of a stoichiometric air/fuel mixture.

To determine the maximum amount of bypass flow, the core mass flow is set to 60kg/s (Belgian F16 Fighting Falcon) and the BPR of the CDFS is increased until the exit Mach number of the AB reaches the critical value 1. This is done for each of the 3 first single bypass simulation points since an increasing trend is detected. The lowest value, - 10 % safety margin, is set and the SLS thrust is calculated to see if it reaches the minimum of 150kN. If this is not the case, the core mass flow will be increased and everything retested.
The values of the PQ are chosen differently for each case since there has not been determined a specific fan PQ yet.

Point	1	2	3
Altitude (m)	0	3048	5029
Mach	0,0	1,0	1,6
$CDFS.BPR_{MAX}$	1,6	1,7	2,0
bypass mass flow (kg/s)	96	102	120

Table 3.6 Maximum bypass mass flow

With the results from table 3.6, the CDFS BPR and core mass flow are determined. Only the front fan PQ and BPR are left from the list of unknowns in paragraph 3.2.

3.4.4 Fan

Last, the fan PQ and BPR are unknown.

The fan PQ has a whole range of possible values but according to [22], the optimum fan pressure ratio is reached when both input speeds in the back mixer are equal. Pay attention: although the speed is the same, Mach numbers can be different since the temperatures are not equal.
Determining the fan maximum BPR is simply done by increasing the BPR until the AB exit Mach number reaches 1 at the Mach 2,6 testing point. At this point the front VABI reaches its maximum opening position and related mass flow according to reference [3].

Fan PQ

To determine the PQ, the engine will be run in single bypass mode and with a fixed PQ and BPR for the CDFS. Single bypass mode and fixed PQ will be used because they enable the possibility of easily calculating the total (tot.) PQ in the bypass channel. A fixed BPR is applied because in this way, no third VABI system is necessary. In double bypass mode, the bypass flow is a mixture of the flow from the fan and CDFS tip so mixing effects should be taken into account for the PQ. This means an extra variable will be used.

- MIN no backflows;
- Optimal (OP) equal input speeds in back mixer;
- MAX just before supersonic flow.

Point	1	2	3
Altitude (m)	0	3048	5029
Mach	0,0	1,0	1,6
Fan PQ_{MIN}	3,3	2,7	2,0
Fan PQ_{OP}	3,6	2,9	2,1
Fan PQ_{MAX}	4,9	4,0	2,8
Tot. PQ_{MIN}	4,6	3,7	2,8
Tot. PQ_{OP}	5,0	4,0	2,9
Tot. PQ_{MAX}	6,8	5,5	3,9

Table 3.7 Possible PQ's in function of test point

Table 3.7 clearly shows there is no fan PQ in this configuration that can serve in every flight position. But since the fan can only have one PQ, a solution has to be found.

In the first place, it was thought to lower the tip PQ by using the VIGV in function of the flight condition (figure 3.10) with a constant fan PQ. This would only mean that the bypass PQ changes while the core PQ stays constant. The latter one should result in a constant PQ for the compressor and related map scaling factors. There are three big problems. First of all, adapting the angle of the VIGV with the eye on changing the PQ will cause stall. Second, differences that are so large are not possible and will also affect the mass flow and efficiency. Last, to cover the whole range of flight conditions, a PQ lower than 1 is necessary. This means the tip will start operating as a turbine what causes whole range of unwanted effects.

Figure 3.10 VIGV [12]

The key to this issue is found in the CDFS BPR. As seen in paragraph 3.4.2, the BPR has no effect on the PQ. But when two mixers are coupled, like in the RTA engine model, the first mixer will affect the second one. For example: a small mass flow with a high PQ will not cause backflows in a lower PQ channel with a high mass flow.

All this means that the PQ problem has become a BPR problem again. Since SLS is one of the most demanding phases of flight and the engine is running in single bypass mode, the optimum fan PQ of 3,6 is taken as the fixed value. Also the BPR of 1,35 will serve as a starting point.
In each test point, the maximum CDFS BPR possible with a fan PQ of 3,6 is searched. The results will be different from table 3.6 since the back mixer becomes a limit instead of the AB now.

Point	1	2	3
Altitude (m)	0	3048	5029
Mach	0,0	1,0	1,6
CDFS BPR_{MAX}	1,5	1,6	0,8

Table 3.8 Maximum BPR CDFS

With the results of table 3.7 and 3.8 the fan PQ is fixed at 3,6. Further, the CDFS BPR is changed from a fixed value to a dynamic one to prevent backflows. This means a third VABI system is needed in the real engine. For the engine model, nothing changes.
The BPR at Mach 1,6, - 10 % safety margin is suggested to be constant above Mach 1,6. Otherwise it is not possible to determine a certain BPR for the fan.

Fan BPR

Just like mentioned above, the fan BPR is calculated at test point 5 since the mass flow reaches its maximum value there.

For the simulations:

- fan PQ 3,6;
- CDFS PQ 1,38;
- CDFS BPR 0,7.

are chosen based on the simulations above.

At Mach 2,6, a maximum fan BPR of 0,32 is possible. Above 0,32 there are variables which are exceeding the subsonic limit, causing converging errors. Pay attention: when a FOR-loop is used, values up to 1,2 are possible. A FOR-loop is using data from the previous point, causing unrealistic values.
When the calculations are done for the Mach 2 test point, a BPR of 0,45 is reached. This means the cross sectional area will reach its maximum at Mach 2 instead of Mach 2,6. The difference with reference [13] can be explained by the suggestion that the BPR of the CDFS is constant when transitioning to double bypass mode.

3.4.5 SLS vs. Mach 2

According to figure 1.15, the Mach 2 test point should be the most demanding phase of flight. To check this statement, the results of the design partition at SLS and Mach 2 are compared.

After the different simulations above, the unknown values from 3.2 are:

- TURBOJET.Altitude depending on test point;
- TURBOJET.Mach depending on test point;
- fan BPR maximum 0,4 at Mach 2;
- fan PQ 3,6;
- CDFS BPR 1,35 – 0,7;
- core mass flow 60kg/s;
- CDFS PQ 1,38.

The results of both design calculations can be seen in table 3.9.

In almost all the cases, the SLS condition is the most demanding or equal to Mach2.
One of the exceptions is the correction factor for the compression work, CG4, from the CDFS and the LPT, these are higher. This means that more work is extracted by the LPT and the CDFS needs more work for the same compression. Logically, the cross sectional area of the second channel in the front mixer, Mixer_F.A2, is bigger at Mach 2 since there is no BPR at SLS. Also the AB area is slightly bigger because the total mass flow increased 1,8 kg/s. Last the cross sectional area for the core input in the back mixer increased to maintain the equilibrium between both static pressures since the other section decreased.

The engine model is already validated with GESTPAN in paragraph 3.3.4, but the values from table 3.9 do not give a good idea whether these values are realistic. Therefore, the diameter is calculated based on the volumes and area's (*A*) in table 3.10. *D* and *d* represent the outer and inner diameter respectively. These values are compared with the dimensions from the P&W F100-220E from the Belgian F16 Fighting Falcon since the core mass flow and rotational speeds are based upon this engine.

To calculate the outer diameter of the front mixer, a compressor diameter of 0,6 is suggested. This results in a maximum of 0,71m and 0,75m for the inner and outer diameter respectively. When the diameter of the output cone after the LPT is set to 0,3, the maximum diameter of the inner and outer channel of the back mixer is 0,75m and 0,87m. Last, an AB diameter of 0,85m is found.
The inlet diameter of the P&W F100-220E is 0,88m which means the engine sizing of the calculated RTA engine model is in the same order. Also the maximum diameter of the bypass channels is almost the same as the AB diameter, which results in an almost cylindrical engine.

	SLS	Mach 2
Fan.CG1	154,672827	83,936338
Fan.CG2	0,909585249	0,909585249
Fan.CG4	508,575352	506,418063
Fan.ND (rpm)	12507,5892	10329,9275
CDFS.tip.CG1	23,5111125	11,2369919
CDFS.tip.CG2	0,978607439	0,907299899
CDFS.tip.CG4	75,5074541	117,28968
CDFS.hub.CG1	17,4156389	16,0528455
CDFS.hub.CG2	0,978607439	0,907299899
CDFS.hub.CG4	75,5074541	117,28968
Mixer_F.A1 (m²)	0,118069962	0,03279669
Mixer_F.A2 (m²)	0	0,037626035
Compressor.CG1	20,9006359	11,1361647
Compressor.CG2	0,909585249	0,909585249
Compressor.CG4	792,374355	384,717849
Compressor.ND (rpm)	11222,6459	9325,42499
Burner.GLP (s/kg)	0,001578202	0,001401653
Burner.VOL (m³)	0,019659585	0,014112919
Turbine_HP.CG1	6,5965731	6,57792294
Turbine_HP.CG2	0,9	0,9
Turbine_HP.CG3	306,412939	306,412939
Turbine_HP.CG4	243,668479	191,074405
Turbine_LP.CG1	16,8901199	13,516264
Turbine_LP.CG2	0,9	0,9
Turbine_LP.CG3	300,761613	293,58195
Turbine_LP.CG4	198,250819	288,966125
Mixer_B.A1 (m²)	0,312195539	0,368439887
Mixer_B.A2 (m²)	0,15138111	0,067051361
AfterBurner.A (m²)	0,562523142	0,573243997
Nozzle_Var.A_exit (m²)	0,529062537	0,501759542

Table 3.9 SLS vs. Mach 2 design

	Mixer_F.A1		Mixer_F.A2		Mixer_B.A1		Mixer_B.A2		AfterBurner.A	
	SLS	Mach 2	SLS	Mach 2	SLS	Mach 2	SLS	Mach 2	SLS	Mach 2
A (m²)	0,12	0,03	0,00	0,04	0,31	0,37	0,15	0,07	0,56	0,57
d (m)	0,60	0,60	0,71	0,71	0,30	0,30	0,75	0,75	0,00	0,00
D (m)	0,71	0,63	0,71	0,75	0,70	0,75	0,87	0,80	0,85	0,85

Table 3.10 Engine dimensions

Based on the schematics of the P&W, the burner dimensions are calculated as well. This volume is also in the same order as the results from the RTA engine model.

The engine delivers a SLS thrust of 159 517N (= specific impulse of 2137s) which is higher then the minimum of 150 000N.
At Mach 2 the design thrust is even higher, 161 429N.

With these results the RTA engine model is designed.
SLS is identified as the most demanding phase except for the LPT and CDFS. If these results are combined with those of the SLS condition, everything is fixed to proceed to transient simulations. Even the maximum mixer areas are known.
A whole range of parameters can still be simulated to investigate the behaviour in function of the flight trajectory but such simulations would outrun the core goal of this project.

4 Future considerations

Since this project is just an initial step simulating the RTA in EcosimPro, there are a lot of future considerations. Below, the considerations are split between the modelling and simulation part.

4.1 Modelling

4.1.1 Inlet

During the composition of the inlet, a lot of suggestion are made. Besides it is one of the most adapted components, this results in the fact that there is still a lot of future work possible.
First of all, it can be interesting to investigate if this sort of conical inlet is the most suitable configuration for this type of engine. Here a 2 shock conical inlet is chosen based on the P&W J58 but the Ram Recovery (RR) of a 3 shock inlet will possibly be better. Or would a rectangular inlet with variable ramps be the way to go?
Even when the actual function is used there are some improvements possible. The function suggest there is no cone compression which means a shock will take place when $M_0 = 1$. With cone compression this will be somewhat earlier. Also between the shocks, the cone compression will affect the input parameters for the normal shock function. A more precise pressure calculation method will improve the accuracy and maybe the calculated results can be stored to fasten future calculations. Additionally, the spillage can be taken into account when the oblique shock is not at the inlet edge and the cone position could be an extra output variable. Last, calculating the influence of the angle of attack can be interesting for very steep trajectories although it will not make sense for the long level flights of a normal commercial airliner.

4.1.2 CDFS

Since the CDFS is composed with standard EcosimPro components, there are not so many elements which may need some improvements.
A small perfection can be done by implementing the scalar for the flow compression and efficiency of the core flow. Also the default inertial moment should be replaced by a better value based on design dimensions.
In addition some functions can be written within the compressor components to work with VIGV. This could be done just like in GasTurb. Here the deviations for the mass flow, PQ and efficiency are set for a change of 1° of the VIGV. Of course, this will only have an effect on the off-design studies.

4.1.3 VABI's

The possible improvements of the VABI's mainly affect the off-design simulations.
Within the design studies the maximum cross sectional area is calculated by means of mixers. When in off-design, the VABI will decrease the area of these channels and regulate the static pressure.
This means the effect of the valve position on the static pressure needs to be investigated. The aft valve losses need to be calculated as well.

4.1.4 General

Some of the general improvements possible for the total engine model:

- Convergent/divergent nozzle;
- Non-default compressor/turbine maps;
- Non-default inertial moments;
- H_2-fuel capable;
- … .

4.2 Simulation

First of all, some data from the tests of the RTA-1 should have a large positive effect on the results of the simulations. These values can be used to set realistic boundaries in the design partition.
A second improvement can be obtained when the engine operation of the VCE-214 from reference [20] is used. This is an engine based on the RTA-1, changed to fit the LAPCAT mission profile. This engine uses an adapted trajectory as well, which is much more interesting than the TSTO-trajectory. Switching to this trajectory without adapting the engine operation would most likely be very ineffective.
For the transient simulations there are whole range of possibilities and freedoms. Wind milling states, blocked VABI's, mode transition, supercruise, … can be simulated.

It is very clear that there is still a vast amount of possibilities concerning the simulations. These simulations are however nothing without a good and valid engine model. For this reason, most of the time and study should be focussed on the modelling of the engine. Simulating the engine is just peanuts when realistic engine data are available!

Conclusions

The purpose of this project was to model and simulate the RTA in EcosimPro as good as possible.

Two new components are made to model the engine in the first phase: a supersonic conical inlet and a CDFS.
The conical inlet is based on a function to calculate an oblique shock past a cone and a normal shock, both self written functions. With these functions, a two-shock inlet is composed, an oblique shock followed by a normal one, which suggests that there is no oblique shock spillage at the inlet edge, no cone compression and zero angle of attack. Furthermore, the component is tested on the classic gas behaviour for shock conditions. Despite the small deviations for the oblique shock function from the NASA reference tables, the total component reached to high differences in comparison to the suspected pattern. Possibly caused by the simplified pressure calculation method and a larger integration step. Therefore the less dynamic and more ideal NASA tables are used to prevent the deviations from having a large effect on the future calculations.
Second, a CDFS is made with standard EcosimPro components. After the automatically written code is adapted to fit the requirements and to solve some simulations problems, the component is tested and act just like expected.

In a first phase, the total engine model is compared with a similar engine in another simulation tool which delivered results in the same order. Second some small simulations are executed along the RTA's standard TSTO-trajectory to resolve the whole load of totally unknown values like the fan BPR&PQ, CDFS BPR&PQ and core mass flow. First, a separate mixer is simulated to test the influence of the speed bound M1 of channel 1 on the possible pressure ratio between both input channels. An increasing trend of the range with increasing M1 is shown where the actual pressure, temperature, mass flow and mass flow difference between both channels have no effect. Second the CDFS BPR is determined with the critical AB output speed for every single bypass mode point of the trajectory. The lowest value - 10 % safety margin is set as a static BPR since the PQ of the bypass flow is only a function of M1. The core mass flow is based on the P&W F100-220E from the Belgian F16 Fighting Falcon and the total thrust is calculated to check if the minimum of 150kN is reached. Next the possible fan PQ's are tested for every point of the single bypass mode trajectory. These simulations showed that there is no overall fan PQ possible in this configuration to operate at every flight condition. This resulted in the change of the CDFS BPR from a static to a dynamic value. The mass flow had no effect on a single mixer but when both mixers are coupled, a decreasing BPR results in an increasing fan PQ. All this resulted in a fixed fan PQ which is optimized for the SLS condition since this is one of the most demanding phases of flight. All this means that a third VABI system is needed instead of the formerly suggested two.
The maximum fan BPR is determined in the suggestion that the CDFS BPR stays constant when switching to double bypass mode. Again, the maximum BPR is limited by the critical value of the AB output speed.
Last the results of the SLS and Mach 2 design partitions are compared to see if Mach 2 is the most demanding phase of flight based on our suggestions. Despite of some operation related parameters, the SLS condition is found to be the most demanding phase of flight.

The difference with the related RTA papers can be explained with the suggestions which are made during the whole modelling and simulation of the model.

As an overall conclusion can be said that is was possible to model and to simulate the RTA in EcosimPro. New components were made and a lot of unknown parameters are determined with separate simulations and their physical limitations. Some suggestions are made during the modelling and the simulations but the total model can be improved with the considerations in chapter 4.

References

[1] *Het Von Karman Instituut, een briesje voor de wetenschap*. Retrieved the 26th of February 2009, from http://www.hangarflying.be/index.php?action=view&id=40&module=newsmodule&src=%40random4780e4aaba578.

[2] *The von Karman Institute for fluid dynamics.* Retrieved the 26th of February 2009, from http://www.vki.ac.be/index.php?option=com_content&view=frontpage&Itemid=1.

[3] McNelis, N., Bartolotta, P. (2005). Revolutionary Turbine Accelerator (RTA) Demonstrator (AIAA 2005-3250). *13th International Space Plane and Hypersonic Systems and Technologies.* Reston: AIAA.

[4] Heitmeir, F.J. (1995). Combined-Cycle engines for hypersonic applications. In: AGARD; *Advanced Aero Engine Concepts and Controls* (16). Neuilly-sur-Seine: AGARD.

[5] Oggero, L., Pilidis, P. (1998). A novel optimisation method for variable cycle engines (ASME 98-GT-142). New York: ASME.

[6] Pedersen, G.H. (1977). Variable cycle gas turbine engine (US Patent 4,054,030).

[7] Wagenknecht, C.D., Faust, G.K. (1979). Individual bypass injector valves for a double bypass variable cycle turbofan engine (US Patent 4,175,384).

[8] *SR-71 Blackbird.* Retrieved the 13th of May 2009, from http://www.nasa.gov/centers/dryden/news/FactSheets/FS-030-DFRC.html.

[9] Bartolotta, P.A., McNelis, N.B., Shafer, D.G. (2003). High Speed Turbines: Development of a Turbine Accelerator (RTA) for Space Access (AIAA 2003-6943). *12th AIAA International Space Planes and Hypersonic Systems and Technologies*. Norfolk. Reston: AIAA.

[10] Johnson, J.E. (1995). Variable Cycle Engine Concepts. In: AGARD; *Advanced Aero Engine Concepts and Controls* (16). Neuilly-sur-seine: AGARD.

[11] Lee, J., Winslow, R., Buehrle, R.J. (2005). The GE-NASA RTA hyperburner design and development (NASA/TM-2005-213803). *40th Combustion, 28th Airbreathing Propulsion, 22nd Propulsion Systems Hazards, 4th Modeling and Simulations Joint Subcommittees Meetings*. South Carolina: NASA.

[12] Johnson, J.E. (1998). Turbofan engine with a core driven supercharged bypass duct and fixed geometry nozzle (US Patent 5,806,303).

[13] Davoudzadeh, F., Buehrle, R.J., Liu, N., Winslow, R. (2005). Numerical simulation of the RTA combustion rig (NASA/TM-2005-213899). *40th Combustion, 28th Airbreathing Propulsion, 22nd Propulsion Systems Hazards, 4th Modeling and Simulations Joint Subcommittees Meetings*. South Carolina: NASA.

[14] Steelant, J. (2008). LAPCAT: High-Speed Propulsion Technology. In *Advances on Propulsion Technology for High-Speed Aircraft* (pp. 12-1 – 12-38). Neuilly-sur-Seine: RTO.

[15] *Gas Turbine Performance.* Retrieved the 27th of April, from http://www.gasturb.de/.

[16] *GSP - Gas Turbine Simulation Program.* Retrieved the 27th of April , from http://www.gspteam.com/main/main.shtml.

[17] Emanuel, G. (1986). *Gasdynamics, theory and applications*. New York: AIAA.

[18] Jacques, R.J. (1990). *Toegepaste mechanica turbomotoren. Onderdelen, sturing, regeling*. Un-published course. Brussel: KMS.

[19] Sims, J.L. (1964). Tables for supersonic flow around right circular cones at zero angle of attack (NASA SP-3004). Washington: NASA.

[20] Sippel, M. (2006). Research on TBCC Propulsion for a Mach 4.5 Supersonic Cruise Airliner (AIAA 2006-7976). *14th AIAA Space Planes and Hypersonic Systems and Technologies Conference*. Reston: AIAA.

[21] Grönstedt, T. (2000). *Development of methods for analysis and optimization of complex jet engine systems*. Un-published doctoral thesis. Göteborg: Chalmers University of Technology.

[22] Guha, A. (2001, September-October). Optimum Fan Pressure Ratio for Bypass Engines with Separate or Mixed Exhaust Streams. *Journal of Propulsion and Power*, 17(5), 1117-1122.

[23] (2008). *EcosimPro. Modelling and Simulation Software. Installation & Getting Started Guide. Version 4.4* [PDF]. Madrid: EA Internacional.

[24] (2008). *EcosimPro. Modelling and Simulation Software. User Manual. Version 4.4* [PDF]. Madrid: EA Internacional.

[25] (2008). *EcosimPro. Modelling and Simulation Software. EL Modelling Language. Version 4.4* [PDF]. Madrid: EA Internacional.